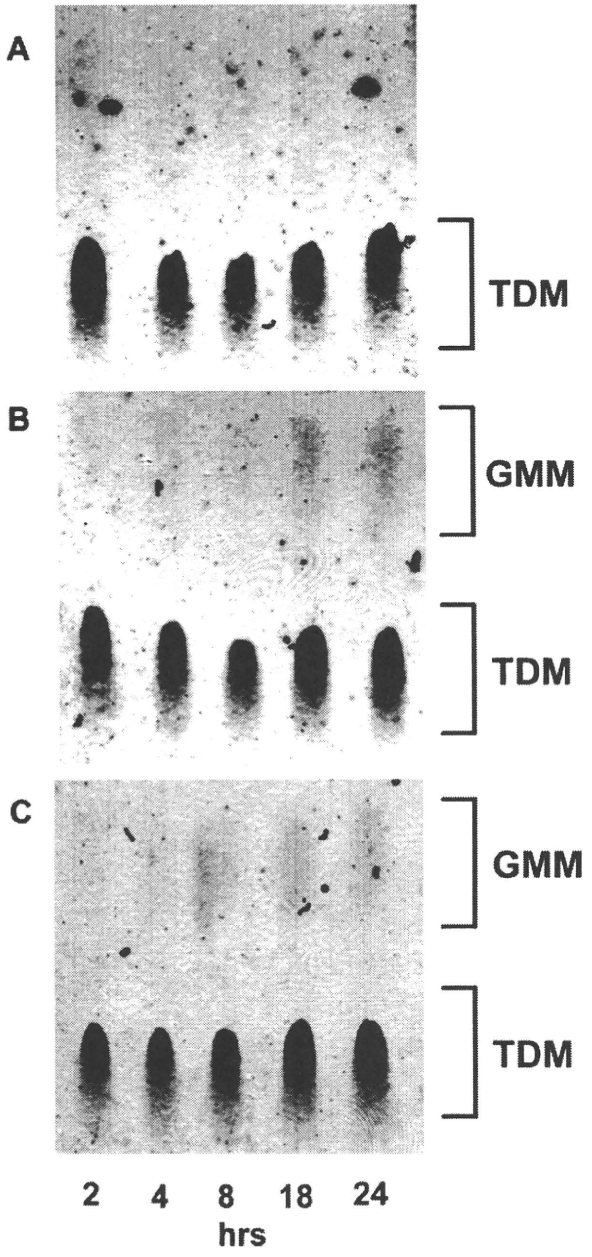

FIGURE 5. **GMM production by mycobacteria during early phases of culture.** MAC was cultured either in liquid media containing 0.01% (*A*) or 0.1% (*B*) glucose or in human serum (*C*). At indicated time points, the bacteria were harvested, and the total lipids were analyzed by TLC.

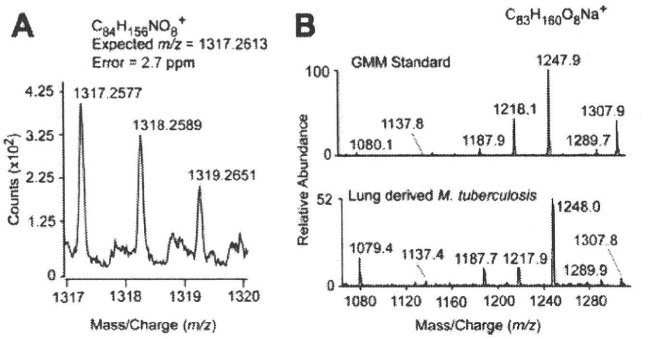

FIGURE 6. **GMM production *in vivo* by *M. tuberculosis*.** *A*, among the mixture of lipids extracted from *M. tuberculosis* derived from mouse lungs, lipids that copurified with a GMM standard were analyzed in the positive mode on an Accurate Mass QTOF MS. The detected mass of *m/z* 1317.2577 corresponds to the predicted mass of an ammonium adduct of C_{78} GMM (*m/z* 1317.2613). *B*, positive mode CID-MS analysis in ion trapping mass spectrometry of *M. fallax* GMM and the lung-derived candidate GMM molecule detected as sodium adducts show a similar pattern of product ions.

sized as a series of molecules that differ from one another by mass increments corresponding to C_2H_2, and the spectrum of the lung-derived lipids contained two additional ions (*m/z* 1345.3033, 1289.2304) corresponding to the expected masses of C_{80} and C_{76} GMM (data not shown). Finally, a separate CID-MS experiment, carried out with an *M. fallax* GMM standard and the lung-derived lipids, showed nearly identical product ions, including ions with mass intervals corresponding to the loss of 60, 90, and 120 units (*m/z* 1248.0, 1217.9, and 1187.7), which likely represent the loss of $C_2H_4O_2$, $C_3H_6O_3$, and $C_4H_8O_4$, which are products expected from cleavage through the hexose sugar (Fig. 6*B*). These data provide strong evidence that GMM is made in the host *in vivo* during an experimental infection.

DISCUSSION

MAC represents a group of environmental mycobacteria that have evolved the capacity to adapt to low nutrition environments. In fact, MAC can survive and replicate in water supply systems (1), where aggregates of the microbes exist in close association with the surface area. This biofilm formation confers significant resistance to a variety of physical and chemical stresses, such as exposure to disinfectants and antibiotics, and thus is an important strategy for the environmental mycobacteria to maintain their life cycles safely in natural environments. These environmental mycobacteria stably express TDM on the surface of their cell wall but fail to biosynthesize GMM because of highly limited availability of glucose. This study argues that, upon entry into the host, this glycolipid phenotype would be modified enzymatically by utilizing the host-derived glucose as a substrate. All three functional mycolyltransferases (Ag85A, Ag85B, and Ag85C) identified in *M. tuberculosis* (18) appear capable of catalyzing TDM synthesis from TMM *in vitro*, and the corresponding Ag85 isoforms have been found also in *M. avium*. Although these enzymes have certain overlapping functions, their differential transcription patterns have been noted in mycobacteria grown under distinct conditions. Ag85A is an isoform that is preferentially expressed in macrophage-resident mycobacteria (19, 20), and thus, its catalytic potential for the TDM-GMM exchange could have an impact on macrophage functions if TDM and GMM have differential ability to activate the cells. Indeed, we recently found that interferon-γ-primed macrophages produced only a marginal level of nitric oxides when stimulated with GMM, which contrasted sharply with those stimulated with TDM that were capable of mounting robust nitric oxide responses (data not shown). Therefore, the TDM-GMM exchange may be valuable in minimizing the nitric oxide response by the host macrophages. Prior to this report, the identity of any mycolyltrans-

ferase that could produce GMM was unknown, so these results establish that Ag85A has this function.

Once pathogens break the frontline defense mediated by the host innate immunity, they are then challenged by specific T lymphocytes that belong to the acquired immunity. Glycolipid-specific T lymphocyte reactions are elicited in humans and guinea pigs infected with mycobacteria, and activation of these T cells is restricted not by the classical major histocompatibility complex-encoded class I and class II molecules but rather by nonmajor histocompatibility complex-encoded group 1 CD1 molecules (CD1a, CD1b, and CD1c in humans) (21). These CD1 molecules are expressed in activated macrophages as well as dendritic cells, the two major cell types for mycobacterial infection. Notably, infiltration of GMM-specific, CD1b-restricted T cells is detected in human skin infected with *M. leprae*, and the human T cell lines (7) and polyclonal T cells (22) exhibit cytotoxic effects, suggesting that the CD1-restricted T cell response directed against GMM could potentially function to clear infection. Taken together, these results raise an interesting possibility that GMM generated as a result of TDM-GMM exchange functions to reduce the innate immune response, but provides the host with a new opportunity to monitor live mycobacteria and eliminate them in the subsequent phases of the acquired immunity. This may represent an example of how the immune system has been constructed during the long processes of evolution to fight efficiently against pathogens.

Despite the fact that GMM is produced by pathogenic mycobacteria and structurally related to the well studied TDM, it has not been the target for focused investigation until recently. Presumably, this is partly because only a tiny amount of GMM, as compared with TDM, is synthesized by pathogenic slow growing mycobacteria, such as *M. tuberculosis* and *M. avium*, when cultured in the Middlebrook "standard" media formulations. Ironically, the standard media used for cultivation of fast growing saprophytic bacteria, such as *Rhodococcus ruber*, contain 1% glucose, and thus, the nonpathogenic bacteria cultured in such a medium produce GMM abundantly, and its structure and biological activities have been studied extensively (6, 23). In many previous studies, the composition, structure, and function of mycobacterial lipids were determined by using bacteria grown in standard media, but the present study suggests that the "lipid world" that is constructed by the bacteria grown in standard culture conditions is substantially different from the lipid world constructed as a result of interaction with the continuously changing host environments.

Acknowledgments—We thank Dr. Seiko Mizuno (Soai University, Osaka, Japan) for use of the GC-MS facility and Dr. Tan-Yun Cheng (Brigham and Women's Hospital, Harvard Medical School, Boston, MA) for reagents and advice.

REFERENCES

1. Primm, T. P., Lucero, C. A., and Falkinham, J. O., III (2004) *Clin. Microbiol. Rev.* **17,** 98–106
2. Sathyamoorthy, N., and Takayama, K. (1987) *J. Biol. Chem.* **262,** 13417–13423
3. Ryll, R., Kumazawa, Y., and Yano, I. (2001) *Microbiol. Immunol.* **45,** 801–811
4. Brennan, P., and Ballou, C. E. (1967) *J. Biol. Chem.* **242,** 3046–3056
5. Moody, D. B., Guy, M. R., Grant, E., Cheng, T. Y., Brenner, M. B., Besra, G. S., and Porcelli, S. A. (2000) *J. Exp. Med.* **192,** 965–976
6. Matsunaga, I., Oka, S., Inoue, T., and Yano, I. (1990) *FEMS Microbiol. Lett.* **55,** 49–53
7. Moody, D. B., Reinhold, B. B., Guy, M. R., Beckman, E. M., Frederique, D. E., Furlong, S. T., Ye, S., Reinhold, V. N., Sieling, P. A., Modlin, R. L., Besra, G. S., and Porcelli, S. A. (1997) *Science* **278,** 283–286
8. Matsunaga, I., Bhatt, A., Young, D. C., Cheng, T. Y., Eyles, S. J., Besra, G. S., Briken, V., Porcelli, S. A., Costello, C. E., Jacobs, W. R., Jr., and Moody, D. B. (2004) *J. Exp. Med.* **200,** 1559–1569
9. Enomoto, Y., Sugita, M., Matsunaga, I., Naka, T., Sato, A., Kawashima, T., Shimizu, K., Takahashi, H., Norose, Y., and Yano, I. (2005) *Biochem. Biophys. Res. Commun.* **337,** 452–456
10. Kremer, L., Maughan, W. N., Wilson, R. A., Dover, L. G., and Besra, G. S. (2002) *Lett. Appl. Microbiol.* **34,** 233–237
11. Cheng, T. Y., Relloso, M., Van Rhijn, I., Young, D. C., Besra, G. S., Briken, V., Zajonc, D. M., Wilson, I. A., Porcelli, S., and Moody, D. B. (2006) *EMBO J.* **25,** 2989–2999
12. Grant, E. P., Degano, M., Rosat, J. P., Stenger, S., Modlin, R. L., Wilson, I. A., Porcelli, S. A., and Brenner, M. B. (1999) *J. Exp. Med.* **189,** 195–205
13. Sugita, M., Porcelli, S. A., and Brenner, M. B. (1997) *J. Immunol.* **159,** 2358–2365
14. Barry, C. E., III, Lee, R. E., Mdluli, K., Sampson, A. E., Schroeder, B. G., Slayden, R. A., and Yuan, Y. (1998) *Prog. Lipid. Res.* **37,** 143–179
15. Natsuhara, Y., Oka, S., Kaneda, K., Kato, Y., and Yano, I. (1990) *Cancer Immunol. Immunother.* **31,** 99–106
16. Anderson, D. H., Harth, G., Horwitz, M. A., and Eisenberg, D. (2001) *J. Mol. Biol.* **307,** 671–681
17. Ohara, N., Matsuo, K., Yamaguchi, R., Yamazaki, A., Tasaka, H., and Yamada, T. (1993) *Infect. Immun.* **61,** 1173–1179
18. Belisle, J. T., Vissa, V. D., Sievert, T., Takayama, K., Brennan, P. J., and Besra, G. S. (1997) *Science* **276,** 1420–1422
19. Hou, J. Y., Graham, J. E., and Clark-Curtiss, J. E. (2002) *Infect. Immun.* **70,** 3714–3726
20. Mariani, F., Cappelli, G., Riccardi, G., and Colizzi, V. (2000) *Gene (Amst.)* **253,** 281–291
21. Matsunaga, I., and Sugita, M. (2007) *Curr. Immunol. Rev.* **3,** 145–150
22. Ulrichs, T., Moody, D. B., Grant, E., Kaufmann, S. H., and Porcelli, S. A. (2003) *Infect. Immun.* **71,** 3076–3087
23. Matsunaga, I., Oka, S., Fujiwara, N., and Yano, I. (1996) *J. Biochem. (Tokyo)* **120,** 663–670

Biochemical and Biophysical Research Communications 377 (2008) 889–893

Contents lists available at ScienceDirect

Biochemical and Biophysical Research Communications

journal homepage: www.elsevier.com/locate/ybbrc

Trans-species activation of human T cells by rhesus macaque CD1b molecules

Daisuke Morita [a,b], Kumiko Katoh [a,b], Toshiyuki Harada [c], Yoshiaki Nakagawa [c], Isamu Matsunaga [a,b], Tomoyuki Miura [d], Akio Adachi [e], Tatsuhiko Igarashi [d,*], Masahiko Sugita [a,b,*]

[a] Laboratory of Cell Regulation, Institute for Virus Research, Kyoto University, 53 Kawahara-cho, Shogoin, Sakyo-ku, Kyoto 606-8507, Japan
[b] Laboratory of Cell Regulation and Molecular Network, Graduate School of Biostudies, Kyoto University, Kyoto 606-8501, Japan
[c] Division of Applied Life Sciences, Graduate School of Agriculture, Kyoto University, Kyoto 606-8502, Japan
[d] Laboratory of Primate Model, Institute for Virus Research, Kyoto University, Kyoto 606-8507, Japan
[e] Department of Virology, Institute of Health Biosciences, The University of Tokushima Graduate School, Tokushima 770-8503, Japan

ARTICLE INFO

Article history:
Received 11 October 2008
Available online 23 October 2008

Keywords:
Rhesus macaque
CD1
Mycobacteria
Glucose monomycolate

ABSTRACT

Despite crucial importance of non-human primates as a model of human infectious diseases, group 1 CD1 genes and proteins have been poorly characterized in these species. Here, we isolated *CD1A*, *CD1B*, and *CD1C* cDNAs from rhesus macaque lymph nodes that encoded full-length CD1 proteins recognized specifically by monoclonal antibodies to human CD1a, CD1b, and CD1c molecules, respectively. The monkey group 1 CD1 isoforms contained amino acid residues and motifs known to be critical for intramolecular disulfide bond formation, N-linked glycosylation, and endosomal trafficking as in human group 1 CD1 molecules. Notably, monkey CD1b molecules were capable of presenting a mycobacterial glycolipid to human CD1b-restricted T cells, providing direct evidence for their antigen presentation function. This also detects for the first time a trans-species crossreaction mediated by group 1 CD1 molecules. Taken together, these results underscore substantial conservation of the group 1 CD1 system between humans and rhesus macaque monkeys.

Besides MHC class I- and II-restricted αβ T cells that recognize protein antigens (Ags), discrete subsets of T cells exist in humans that specifically recognize non-protein Ags in a T-cell receptor (TCR)-dependent manner. These include αβ T cells that recognize lipid, glycolipid, and lipopeptide Ags in the context of group 1 CD1 molecules (CD1a, CD1b, and CD1c) as well as $V\gamma2^{+}V\delta2^{+}$ γδ T cells that recognize pyrophosphorylated isoprenoid intermediates [1,2]. Both T cell subsets have been implicated in host defense against mycobacterial infection [3], and therefore, animal species that have evolved these T cells in addition to MHC-restricted T cells would serve as an ideal animal model of human tuberculosis. The murine model has long been studied extensively, and by taking advantage of versatile genetic manipulation and a fine array of reagents, many important aspects of host defense against tuberculosis have been demonstrated explicitly, that include a critical role for MHC-restricted T cells [4]. However, a significant difference in pathology has been noted between the two species [3], and the lack of T cells in mice that correspond to human group 1 CD1-resricted T cells and $V\gamma2^{+}V\delta2^{+}$ γδ T cells makes the animals less useful particularly in an attempt to develop a new chemical class of non-protein vaccines against tuberculosis. In contrast to mice and rats, guinea pigs exhibit pathology that is comparable, if not identical, to that in human tuberculosis, and recent studies have shown that they contain four *CD1B* genes and three *CD1C* genes [5,6]. Nevertheless, CD1a-restricted T cells as well as CD1d-restricted NKT cells may not exist in guinea pigs. These and other significant differences in the organization and function of the immune system between humans and rodents often make it difficult to translate the results obtained from rodent models to humans. Further, certain human pathogens, such as HIV-1, exhibit highly limited host selectivity, and are unable to infect into rodents and other commonly used laboratory animals.

Recently, the value of non-human primates as a model of human infectious diseases has been appreciated greatly for elucidating pathogenesis and for developing vaccines and therapies against microbial infections, such as AIDS and tuberculosis [7,8]. Nevertheless, little has been defined about the genes, proteins, and function of the group 1 CD1 molecules in non-human primates, and therefore, the present study was aimed at identifying the rhesus macaque group 1 CD1 system. We found it highly comparable to that in humans, and rhesus macaque CD1b molecules were indeed able to present a human CD1b-presented mycobacterial glycolipid Ag to specific human T cells.

* Corresponding authors. Fax: +81 75 752 3232 (M. Sugita), +81 75 761 9335 (T. Igarashi).
E-mail addresses: tigarash@virus.kyoto-u.ac.jp (T. Igarashi), msugita@virus.kyoto-u.ac.jp (M. Sugita).

0006-291X/$ - see front matter © 2008 Elsevier Inc. All rights reserved.
doi:10.1016/j.bbrc.2008.10.075

Materials and methods

Isolation of rhesus macaque group 1 CD1 cDNAs. Rhesus monkeys (*Macaca mulatta*) were used in accordance with the institutional regulations approved by the Committee for Experimental Use of Nonhuman Primates of the Institute for Virus Research, Kyoto University, Kyoto, Japan. Total RNA was extracted from rhesus macaque lymph nodes using the RNeasy mini kit (Qiagen, Hilden, Germany), and the first-strand cDNA was synthesized from 0.5 mg of the total RNA using oligo(dT) and PrimeScript reverse transcriptase (Takara Bio, Inc., Otsu, Japan). To amplify specific transcripts, the samples were subjected to PCR amplification with *Pfu* DNA polymerase (Stratagene, La Jolla, CA) for 35 cycles of 30 s at 94 °C, 1 min at 55 °C (for *CD1A*) or 60 °C (for *CD1B* and *CD1C*), 2 min at 72 °C, and a final cycle of 10 min at 72 °C. The primers used were: 5′-GCG GTA CCA AAT AAC ATC TGC AAA TGA C-3′ (sense) and 5′-GCC TCG AGA AGG AGG ATC ATG GTG TAT C-3′ (anti-sense) for *CD1A*; 5′-GCG GTA CCA GTA AGA AGT TGC ATC TCC C -3′ (sense) and 5′-GCC TCG AGG GAG CAG ACA TGG TGA GGG C-3′ (anti-sense) for *CD1B*; 5′-GCG GGT ACC ACC ATG CTG TTT CTG CAG TTT-3′ (sense) and 5′-GCG GCG GCC GCA TTG TAC TAG GCT CCT GG-3′ (anti-sense) for *CD1C*. The PCR products were purified and cloned into pcDNA3.1(+) (Invitrogen, Carlsbad, CA), and DNA sequencing was done in both directions. This procedure was repeated twice to confirm that no PCR-associated errors were introduced.

Transfection. A rhesus macaque kidney epithelial cell line, LLC-MK2 [9], was obtained from ATCC (Manassas, VA). The cells were transfected with pcDNA3.1(+) containing either rhesus macaque *CD1A*, *CD1B*, or *CD1C* by a calcium phosphate precipitation method, using the mammalian transfection kit (Stratagene). The transfected cells were then cultured in DMEM media (Invitrogen) supplemented with 10% fetal calf serum (Hyclone, Logan, UT) and G418 (0.5 mg/ml) (Invitrogen), and the CD1-expressing cells were then enriched by labeling with specific antibodies (Abs), followed by positive selection with magnetic beads coated with goat anti-mouse IgG Abs (Invitrogen). A human lymphoblastoid cell line, T2 [10], was transfected with pCEP4 (Invitrogen) containing *CD1A* or *CD1B* of either human or rhesus macaque origin by electroporation as described [11], followed by selection in RPMI1640 media (Invitrogen) containing 0.2 mg/ml hygromycin B (Invitrogen). A human cervical epithelial cell line, HeLa [12], was transfected with rhesus macaque *CD1C* in pcDNA3.1(+) by a calcium phosphate precipitation method, and selection was performed as described above. These stably transfected cells were used as Ag-presenting cells (APCs) in T cell transfectants stimulation assays.

Flow cytometry. The expression of CD1 proteins on the surface of the LLC-MK2 cell transfectants as well as rhesus macaque thymocytes were analyzed by flow cytometry as described [13,14], using the BD FACSCanto II flow cytometer. The mouse monoclonal Abs (mAbs) used were 10H3 (anti-human CD1a) [15], SN13 (anti-human CD1b) (Ancell, Bayport, MN), M241 (anti-human CD1c) (Ancell), and SP34 (anti-monkey CD3) (BD Biosciences, Franklin Lakes, NJ). MAbs MOPC-31C (BD Biosciences) and RPC5.4 (ATCC) were used as negative controls.

T cell transfectants stimulation assays. TCR-deficient Jurkat cells, J.RT3, reconstituted with either the dideoxymycobactin-specific, CD1a-restricted TCR (J.RT3/CD8-2), the glucose monomycolate (GMM)-specific, CD1b-restricted TCR (J.RT3/LDN5) or the mannosyl phosphomycoketide-specific, CD1c-restricted TCR (J.RT3/CD8-1) have been described previously [16]. The TCR-reconstituted cells (5×10^4/well) were cultured with irradiated APCs expressing a relevant CD1 isoform (1×10^5/well) in wells of 96-well, flat-bottomed microtiter plates (200 μl media/well) in the presence of 10 ng/ml phorbol myristate acetate (PMA) (Sigma, St. Louis, MO) and either the organic extract of *Mycobacterium tuberculosis* H37Ra (for J.RT3/CD8-2 and J.RT3/CD8-1) or *Rhodococcus equi* GMM (for J.RT3/LDN5) at indicated concentrations. After 20 h, aliquots of the culture supernatants were collected, and the amount of interleukin-2 (IL-2) released into the supernatants was measured by the IL-2 ELISA kit (BD Biosciences).

Molecular modeling of rhesus macaque CD1b proteins. Molecular modeling of the rhesus macaque CD1b molecule was performed, using the homology modeling software PDFAMS (Protein Discovery Full Automatic Modeling System; In-Silico Sciences, Inc., Tokyo, Japan) as described [17]. Briefly, the primary sequence of the rhesus macaque CD1b molecule was aligned with the sequence of the human CD1b molecule available from the Protein Data Bank (1UQS), using RPS-BLAST. Amino acid residues differing between the two molecules were mutated, and the obtained 3-dimensional structure was optimized by the simulated annealing method. Subsequently, the molecular model was subjected to energy minimization, using the SYBYL software. The overall structure and the cavity surface of the modeled rhesus macaque CD1b molecule were depicted in association with GMM from *Nocardia farcinica* by utilizing the MOLCAD module of SYBYL.

Results and discussion

Identification of rhesus macaque group 1 CD1 cDNAs

To isolate full-length cDNAs encoding rhesus macaque CD1a and CD1b, the first strand cDNA was synthesized from lymph node total RNA by reverse transcription, and then, PCR was carried out with specific pairs of 5′-end and 3′-end primers that were designed based on the rhesus macaque genomic *CD1A* and *CD1B* sequences. The rhesus macaque genomic *CD1C* sequence was only partially available, and the 3′-end sequence was undermined. Therefore, rhesus macaque *CD1C* cDNA was amplified by PCR using a specific 5′-end primer and a 3′-end primer that was designed based on the sequence of 3′-untranslated region of the human *CD1C* genome. The PCR products thus obtained were of expected size (approximately 1 kb) and the identity of the products was determined by DNA sequences. Identical nucleotide sequences were obtained after two independent PCR amplifications, ruling out the possibility for PCR-associated errors.

Alignment of the deduced amino acid sequences of the putative rhesus macaque *CD1A*, *CD1B*, and *CD1C* genes with the corresponding human CD1 proteins revealed a high-degree homology between the two species (85.6% for CD1a, 94.6% for CD1b, 90.4% for CD1c) (Fig. 1). The cysteine residues (indicated with triangles) involved in the intrachain disulfide bond formation in the α2 and the α3 domains as well as the putative N-linked glycosylation sites (indicated with asterisks) in the α1 and the α2 domains were totally conserved [2]. Further, the cytoplasmic tyrosine-based motif (YXXZ where Y is tyrosine, X is any amino acid, and Z is a hydrophobic amino acid) and its flanking sequences that are known to regulate differential early endosomal and lysosomal trafficking of CD1b and CD1c proteins [12,18,19] were identical between the two species (Fig. 1).

To monitor protein expression of these rhesus macaque *CD1* genes, we first screened mAbs against human CD1 proteins for their cross-reactivity to rhesus macaque thymocytes, a cell type that is presumed to express all forms of group 1 CD1 molecules. As shown in Fig. 2A, mAb clones 10H3 (anti-human CD1a), SN13 (anti-human CD1b), and M241 (anti-human CD1c) labeled a significant fraction of $CD3^{dim}$ thymocytes in a pattern comparable to that for human thymocytes [20]. We then stably transfected each

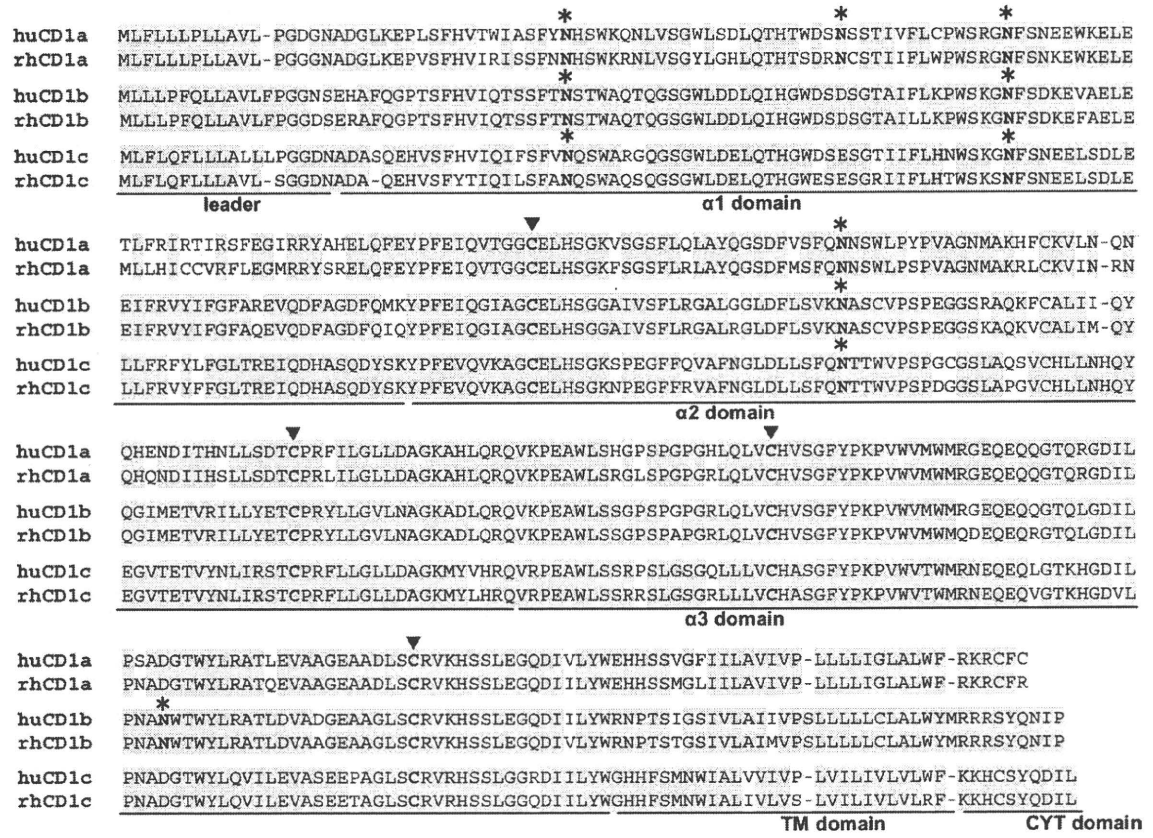

Fig. 1. Alignment of deduced amino acid sequences of human (hu) and rhesus macaque (rh) group 1 CD1 proteins. Residues conserved between the two species are shaded in light gray. Solid triangles denote cysteines conserved in all the group 1 CD1 proteins of both species that are presumed to be involved in intradomain disulfide bond formation. Asterisks indicate potential N-linked glycosylation sites. Dashes represent gaps that have been introduced to maximize alignment. TM domain, transmembrane domain; CYT domain, cytoplasmic domain.

of the putative rhesus macaque *CD1A*, *CD1B*, and *CD1C* genes into a rhesus macaque kidney epithelial cell line, LLC-MK2, and their protein expression was monitored by flow cytometry using the cross-reactive mAbs (Fig. 2B). The 10H3 anti-human CD1a mAb recognized only *CD1A* transfected cells, but not those transfected with the other genes. Similarly, the SN13 anti-human CD1b mAb and the M241 anti-human CD1c mAb showed specific reactivity to cells transfected with the *CD1B* and the *CD1C* genes, respectively. These results provided both evidence for protein expression of the isolated genes and further support for their identity, and therefore, the nucleotide sequences of the putative *CD1A*, *CD1B*, and *CD1C* cDNAs were deposited to the DDBJ/GenBank/EMBL databases as those of rhesus macaque *CD1A* (Accession Nos: AB458511), *CD1B* (AB458512), and *CD1C* (AB458513), respectively.

Trans-species activation of human T cells by rhesus macaque CD1b molecules

With the exception of mice and rats, group 1 CD1 genes have been identified in virtually all mammalian animals so far analyzed, but the Ag presentation function of their products has not been demonstrated so explicitly as in humans [21]. This is partly due to difficulties in obtaining specific T cell lines and clones that recognize lipid Ags in the context of CD1 molecules of a given animal species. Because of the highly conserved amino acid sequences of human and rhesus macaque group 1 CD1 proteins, we considered the possibility that rhesus macaque CD1 molecules might bind lipid Ags that were known to be presented by human CD1 molecules, and interact with specific human TCRs. To address this, human TCRs derived either from a dideoxymycobactin-specific, CD1a-restricted T cell line (CD8-2), from a GMM-specific, CD1b-restricted T cell line (LDN5) or from a mannosyl phosphomycoketide-specific, CD1c-restricted T cell line (CD8-1) were reconstituted in TCR-deficient Jurkat cells (J.RT3) by gene transfer, and the T cell reactivity to specific Ag in the presence of cell transfectants expressing a relevant CD1 isoform of either human or rhesus macaque origin was assessed by measuring IL-2 released from the T cells. J.RT3/CD8-2 cells responded to dideoxymycobactin in the presence of APCs expressing human CD1a molecules, but not those expressing rhesus macaque CD1a molecules (Fig. 3, top panel). Similarly, J.RT3/CD8-1 cells responded to mannosyl phosphomycoketide in the presence of APCs expressing human CD1c molecules, but not those expressing rhesus macaque CD1c molecules (bottom panel). Strikingly, however, APCs expressing rhesus macaque CD1b molecules were capable of presenting GMM efficiently to J.RT3/LDN5 cells (middle panel), providing evidence for their Ag presentation function. The apparently more efficient Ag presentation function for rhesus macaque CD1b molecules as compared with human CD1b molecules could be accounted for by the slightly higher expression on rhesus macaque CD1b transfectants than on human CD1b transfectants (data not shown).

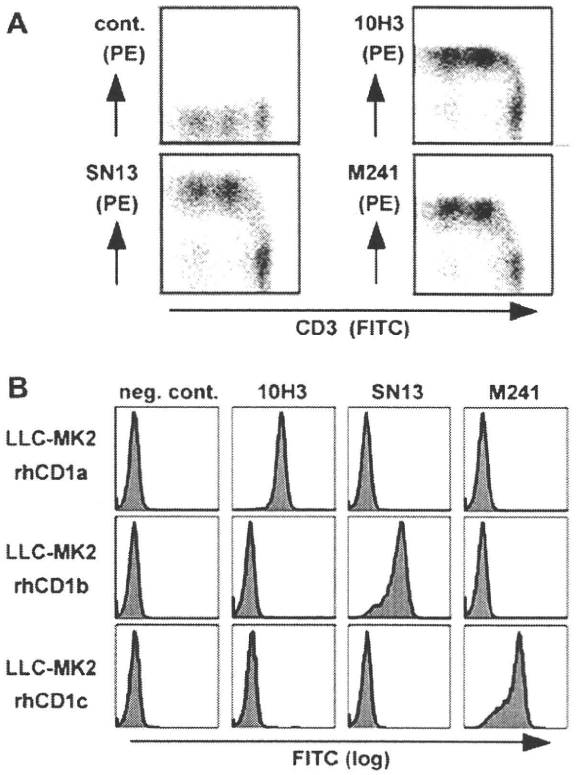

Fig. 2. Cross-reactivity of anti-human CD1 mAbs to rhesus macaque group 1 CD1 proteins. (A) Rhesus macaque thymocytes were double-labeled with the SP34 anti-CD3 mAb and either the 10H3 anti-human CD1a mAb, the SN13 anti-human CD1b mAb, the M241 anti-human CD1c mAb, or negative control Abs, followed by analysis by flow cytometry. (B) A rhesus macaque kidney cell line, LLC-MK2, that stably transfected with either rhesus macaque *CD1A* (LLC-MK2 rhCD1a), *CD1B* (LLC-MK2 rhCD1b), or *CD1C* (LLC-MK2 rhCD1c) were labeled with indicated mAbs and analyzed by flow cytometry.

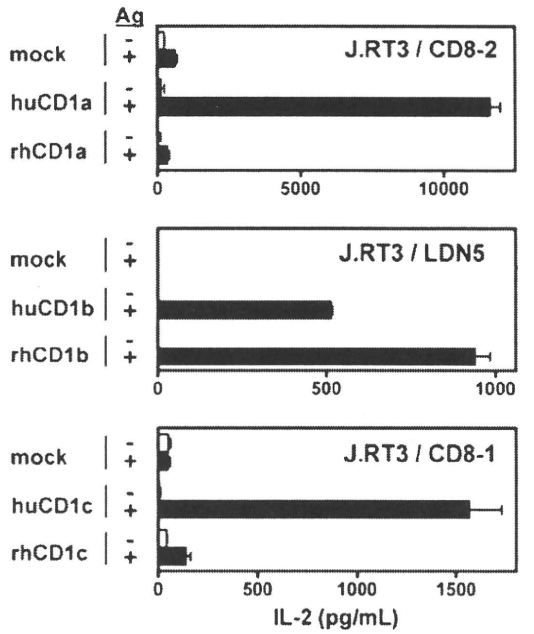

Fig. 3. Ag presentation function of rhesus macaque CD1b molecules. The J.RT3/CD8-2 cells were cultured in the presence or absence of the organic extract of *M. tuberculosis* (50 mg/ml) with T2 cells expressing either human CD1a (huCD1a) or rhesus macaque CD1a (rhCD1a) or those that were mock-transfected (top panel). The J.RT3/LDN5 cells were cultured in the presence or absence of purified GMM (5 mg/ml) with T2 cells expressing either human CD1b (huCD1b) or rhesus macaque CD1b (rhCD1b) or those that were mock transfected (middle panel). The J.RT3/CD8-1 cells were cultured in the presence or absence of the organic extract of *M. tuberculosis* (1.56 mg/ml) with HeLa cells expressing either human CD1c (huCD1c) or rhesus macaque CD1c (rhCD1c) or those that were mock transfected (bottom panel). After 20 h, the culture supernatants were harvested and the amount of IL-2 secreted into the supernatants were measured.

Trans-species crossreaction has never been observed previously for any of the group 1 CD1 molecules. Nevertheless, a molecular model of the rhesus macaque CD1b molecule has detected the α1 and α2 helix structure as well as intramolecular pockets (A′, C′, and F′) and a tunnel (T′) virtually identical to those for human CD1b molecules [22,23], allowing stable interaction with a human CD1b-presented mycobacterial Ag, GMM (Fig. 4). Further, amino acid residues, such as E80 and D83 in the α1 domain and T157 and T165 in the α2 domain, that are proposed to be critical for interaction with specific TCRs [24] are shared between rhesus macaque and human CD1b molecules, suggesting a conserved function for CD1b in these two species. The extent of amino acid sequence conservation is higher in CD1b than in CD1a and CD1c (Fig. 1), which may imply that immune responses to mycolic acid-containing glycolipds are critical for host defense against tuberculosis. So far, no experimental animals have proved extremely useful as a model for studying the group 1 CD1-mediated immunity in human infectious diseases. The present study underscores that monkeys are indispensable for a variety of challenges, including development of a new type of lipid-based vaccines against tuberculosis.

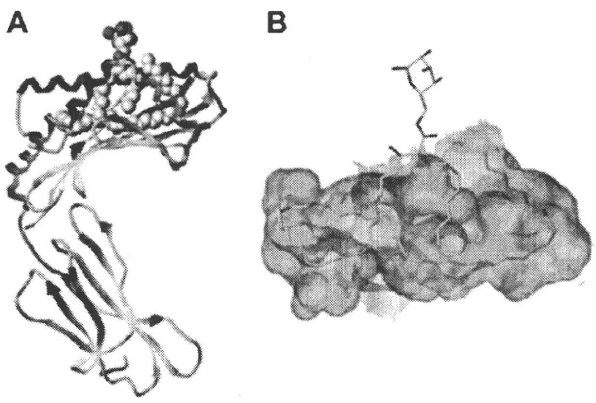

Fig. 4. A molecular model of rhesus macaque CD1b proteins. The rhesus macaque CD1b structure was constructed, based on the crystal structure of the human CD1b-GMM complex. (A) The overall structure of the rhesus macaque CD1b-GMM complex is shown, in which the CD1b heavy chain is depicted in ribbon diagram and the non-hydrogen atoms of GMM are drawn as van der Waals spheres (carbon in gray; oxygen in red). The associated β2-microglobulin is not depicted for simplicity purposes. (B) The binding surface of the Ag-binding groove is drawn in green with the bound GMM in stick (carbon in gray; oxygen in red). (For interpretation of the references to colour in this figure legend, the reader is referred to the web version of this paper).

Acknowledgments

We thank Drs. M. Brenner, D. Olive, and C. Mawas for their gifts of reagents. This work was supported by grants from the Ministry of Education, Culture, Sports, Science and Technology (Grant-in-Aid from Scientific Research on Priority Areas), from the Japan Society for the Promotion of Science (Grant-in-Aid for Scientific Research

(B)), and from the Ministry of Health, Labour, and Welfare (Research on Emerging and Re-emerging infectious Diseases) (to M.S.).

References

[1] C.T. Morita, R.A. Mariuzza, M.B. Brenner, Antigen recognition by human gamma delta T cells: pattern recognition by the adaptive immune system, Springer Semin. Immunopathol. 22 (2000) 191–217.
[2] S.A. Porcelli, The CD1 family: a third lineage of antigen-presenting molecules, Adv. Immunol. 59 (1995) 1–98.
[3] R.J. North, Y.J. Jung, Immunity to tuberculosis, Annu. Rev. Immunol. 22 (2004) 599–623.
[4] T. Mogues, M.E. Goodrich, L. Ryan, R. LaCourse, R.J. North, The relative importance of T cell subsets in immunity and immunopathology of airborne *Mycobacterium tuberculosis* infection in mice, J. Exp. Med. 193 (2001) 271–280.
[5] C.C. Dascher, K. Hiromatsu, J.W. Naylor, P.P. Brauer, K.A. Brown, J.R. Storey, S.M. Behar, E.S. Kawasaki, S.A. Porcelli, M.B. Brenner, K.P. LeClair, Conservation of a CD1 multigene family in the guinea pig, J. Immunol. 163 (1999) 5478–5488.
[6] K. Hiromatsu, C.C. Dascher, M. Sugita, C. Gingrich-Baker, S.M. Behar, K.P. LeClair, M.B. Brenner, S.A. Porcelli, Characterization of guinea-pig group 1 CD1 proteins, Immunology 106 (2002) 159–172.
[7] D.H. Barouch, J. Kunstman, M.J. Kuroda, J.E. Schmitz, S. Santra, F.W. Peyerl, G.R. Krivulka, K. Beaudry, M.A. Lifton, D.A. Gorgone, D.C. Montefiori, M.G. Lewis, S.M. Wolinsky, N.L. Letvin, Eventual AIDS vaccine failure in a rhesus monkey by viral escape from cytotoxic T lymphocytes, Nature 415 (2002) 335–339.
[8] Y. Shen, D. Zhou, L. Qiu, X. Lai, M. Simon, L. Shen, Z. Kou, Q. Wang, L. Jiang, J. Estep, R. Hunt, M. Clagett, P.K. Sehgal, Y. Li, X. Zeng, C.T. Morita, M.B. Brenner, N.L. Letvin, Z.W. Chen, Adaptive immune response of Vgamma2Vdelta2+ T cells during mycobacterial infections, Science 295 (2002) 2255–2258.
[9] R.N. Hull, W.R. Cherry, O.J. Tritch, Growth characteristics of monkey kidney cell strains LLC-MK1, LLC-MK2, and LLC-MK2(NCTC-3196) and their utility in virus research, J. Exp. Med. 115 (1962) 903–918.
[10] M.L. Wei, P. Cresswell, HLA-A2 molecules in an antigen-processing mutant cell contain signal sequence-derived peptides, Nature 356 (1992) 443–446.
[11] M. Sugita, E.P. Grant, E. van Donselaar, V.W. Hsu, R.A. Rogers, P.J. Peters, M.B. Brenner, Separate pathways for antigen presentation by CD1 molecules, Immunity 11 (1999) 743–752.
[12] M. Sugita, X. Cao, G.F. Watts, R.A. Rogers, J.S. Bonifacino, M.B. Brenner, Failure of trafficking and antigen presentation by CD1 in AP-3-deficient cells, Immunity 16 (2002) 697–706.
[13] M. Cernadas, M. Sugita, N. van der Wel, X. Cao, J.E. Gumperz, S. Maltsev, G.S. Besra, S.M. Behar, P.J. Peters, M.B. Brenner, Lysosomal localization of murine CD1d mediated by AP-3 is necessary for NK T cell development, J. Immunol. 171 (2003) 4149–4155.
[14] H. Suzuki, M. Motohara, A. Miyake, K. Ibuki, Y. Fukazawa, K. Inaba, K. Masuda, N. Minato, H. Kawamoto, M. Hayami, T. Miura, Intrathymic effect of acute pathogenic SHIV infection on T-lineage cells in newborn macaques, Microbiol. Immunol. 49 (2005) 667–679.
[15] D. Olive, P. Dubreuil, C. Mawas, Two distinct TL-like molecular subsets defined by monoclonal antibodies on the surface of human thymocytes with different expression on leukemia lines, Immunogenetics 20 (1984) 253–264.
[16] E.P. Grant, M. Degano, J.P. Rosat, S. Stenger, R.L. Modlin, I.A. Wilson, S.A. Porcelli, M.B. Brenner, Molecular recognition of lipid antigens by T cell receptors, J. Exp. Med. 189 (1999) 195–205.
[17] C.E. Wheelock, Y. Nakagawa, T. Harada, N. Oikawa, M. Akamatsu, G. Smagghe, D. Stefanou, K. Iatrou, L. Swevers, High-throughput screening of ecdysone agonists using a reporter gene assay followed by 3-D QSAR analysis of the molting hormonal activity, Bioorg. Med. Chem. 14 (2006) 1143–1159.
[18] M. Sugita, R.M. Jackman, E. van Donselaar, S.M. Behar, R.A. Rogers, P.J. Peters, M.B. Brenner, S.A. Porcelli, Cytoplasmic tail-dependent localization of CD1b antigen-presenting molecules to MIICs, Science 273 (1996) 349–352.
[19] M. Sugita, N. Van Der Wel, R.A. Rogers, P.J. Peters, M.B. Brenner, CD1c molecules broadly survey the endocytic system, Proc. Natl. Acad. Sci. USA 97 (2000) 8445–8450.
[20] L.L. Lanier, J.P. Allison, J.H. Phillips, Correlation of cell surface antigen expression on human thymocytes by multi-color flow cytometric analysis: implications for differentiation, J. Immunol. 137 (1986) 2501–2507.
[21] K. Hiromatsu, C.C. Dascher, K.P. LeClair, M. Sugita, S.T. Furlong, M.B. Brenner, S.A. Porcelli, Induction of CD1-restricted immune responses in guinea pigs by immunization with mycobacterial lipid antigens, J. Immunol. 169 (2002) 330–339.
[22] T. Batuwangala, D. Shepherd, S.D. Gadola, K.J. Gibson, N.R. Zaccai, A.R. Fersht, G.S. Besra, V. Cerundolo, E.Y. Jones, The crystal structure of human CD1b with a bound bacterial glycolipid, J. Immunol. 172 (2004) 2382–2388.
[23] S.D. Gadola, N.R. Zaccai, K. Harlos, D. Shepherd, J.C. Castro-Palomino, G. Ritter, R.R. Schmidt, E.Y. Jones, V. Cerundolo, Structure of human CD1b with bound ligands at 2.3 A, a maze for alkyl chains, Nat. Immunol. 3 (2002) 721–726.
[24] A. Melian, G.F. Watts, A. Shamshiev, G. De Libero, A. Clatworthy, M. Vincent, M.B. Brenner, S. Behar, K. Niazi, R.L. Modlin, S. Almo, D. Ostrov, S.G. Nathenson, S.A. Porcelli, Molecular recognition of human CD1b antigen complexes: evidence for a common pattern of interaction with alpha beta TCRs, J. Immunol. 165 (2000) 4494–4504.

Trehalose Dimycolate Elicits Eosinophilic Skin Hypersensitivity in Mycobacteria-Infected Guinea Pigs[1]

Atsushi Otsuka,*† Isamu Matsunaga,*‡ Takaya Komori,*‡ Kadusa Tomita,*‡ Yoshinobu Toda,§ Toshiaki Manabe,¶ Yoshiki Miyachi,† and Masahiko Sugita[2]*‡

Delayed-type hypersensitivity represents high levels of protein Ag-specific adaptive immunity induced by mycobacterial infection, and can be monitored in the Ag-challenged skin. Besides protein Ags, recent evidence has suggested that a substantial immunity directed against glycolipid Ags is also elicited in response to mycobacterial infection, but skin hypersensitivity to this class of Ags has not been fully assessed. To address this issue directly, glycolipid-specific skin reactions were evaluated in guinea pigs infected with *Mycobacterium avium* complex (MAC). Significant skin induration was observed in MAC-infected, but not mock-infected, guinea pigs, following intradermal administration of a mixture of MAC-derived glycolipids. Surprisingly, this glycolipid-specific skin response involved up-regulated expression of IL-5 mRNA in situ and marked local infiltration of eosinophils. Challenge experiments with individual glycolipid components detected an outstanding capability for trehalose dimycolate (TDM), but not a structurally related glycolipid, glucose monomycolate, to elicit the skin response. T lymphocytes derived from the spleen of MAC-infected, but not uninfected, guinea pigs specifically responded to TDM in vitro by up-regulating IL-5 transcription, and this response was not blocked by Abs that reacted to the known guinea pig group 1 CD1 proteins. Finally, the eosinophilic skin hypersensitivity to TDM was also elicited in guinea pigs vaccinated with bacillus Calmette-Guerin, which contrasted sharply with the classical delayed-type hypersensitivity response to the purified protein derivative. Therefore, the TDM-elicited eosinophilic response defines a new form of hypersensitivity in mycobacterial infection, which may account for local infiltration of eosinophils often observed at the site of infection. ***The Journal of Immunology,*** **2008, 181: 8528–8533.**

Upon infection with mycobacteria, such as *Mycobacterium tuberculosis*, strong Th1 responses to mycobacteria-derived protein Ags are elicited in the majority of immunocompetent individuals, and are expressed in the form of delayed-type hypersensitivity (DTH)[3] (1–3). The Th1-dominant DTH response is thought to be critical for granuloma formation, a pathological process for the host to confine bacteria at the site of infection (4, 5). Failure to elicit the Th1 response often results in inefficient control of mycobacterial infection, as seen in human cases with recessive mutations in genes encoding IFN-γ and IL-12 receptors (6). DTH can be induced at the site of intradermal injection of mycobacteria-derived Ags, and thus, the tuberculin skin test with the purified protein derivative (PPD) is useful for evaluating the protein Ag-specific cellular immunity in the infected host.

Besides protein Ags, recent evidence has suggested that the immune system has evolved the ability to detect microbe-derived glycolipid Ags in innate and adaptive phases of host defense against microbial infection. C-type lectins, such as the macrophage mannose receptor, and Toll-like receptors interact with microbial glycolipids and transmit signals into innate immune cells (7). In addition, CD1-dependent pathways for T cell recognition of microbial glycolipid Ags have also been identified (8–10). The innate and adaptive immune recognition of microbial glycolipid Ags may be particularly important for controlling mycobacterial infection because the lipid-rich cell wall of mycobacteria contains unique glycolipids that are critical for their survival and virulence (11). Indeed, vaccination with *M. tuberculosis*-derived lipids and glycolipids confers protective immunity in the guinea pig model of human tuberculosis, implicating pathways for host defense that are distinct from, but complementary to, those directed against protein Ags (12). Despite the advances in our understanding of immune recognition of mycobacteria-derived glycolipid Ags, skin hypersensitivity reactions to this class of Ags have not been fully assessed. Because of the distinct pathways for host responses to protein and glycolipid Ags, the hypersensitivity response to glycolipids could be substantially different from that directed against protein Ags.

In the present study, we found that trehalose dimycolate (TDM), a major mycolyl glycolipid in the cell wall of mycobacteria, induced hypersensitivity reactions in the skin of *M. avium* complex (MAC)-infected and *M. bovis* bacillus Calmette-Guerin (BCG)-immunized guinea pigs. Notably, the TDM-induced hypersensitivity involved marked infiltration of eosinophils and local expression of IL-5, and thus, was distinct from the protein Ag-induced classical DTH reaction.

*Laboratory of Cell Regulation, Institute for Virus Research, Kyoto University, Kyoto, Japan; †Department of Dermatology, §Center for Anatomical Studies, and ¶Laboratory of Diagnostic Pathology, Graduate School of Medicine, Kyoto University, Kyoto, Japan; and ‡Laboratory of Cell Regulation and Molecular Network, Graduate School of Biostudies, Kyoto University, Kyoto, Japan

Received for publication May 27, 2008. Accepted for publication October 16, 2008.

The costs of publication of this article were defrayed in part by the payment of page charges. This article must therefore be hereby marked *advertisement* in accordance with 18 U.S.C. Section 1734 solely to indicate this fact.

[1] This work was supported by grants from the Ministry of Education, Culture, Sports, Science and Technology (Grant-in-Aid from Scientific Research on Priority Areas) (to M.S.), and from the Japan Society for the Promotion of Science (Grant-in-Aid for Scientific Research (B) (to M.S.) and (C) (to I.M.)).

[2] Address correspondence and reprint requests to Prof. Masahiko Sugita, M.D., Laboratory of Cell Regulation, Institute for Virus Research, Kyoto University, 53 Kawahara-cho, Shogoin, Sakyo-ku, Kyoto, Japan. E-mail address: msugita@virus.kyoto-u.ac.jp

[3] Abbreviations used in this paper: DTH, delayed-type hypersensitivity; BCG, bacillus Calmette-Guerin; MAC, *Mycobacterium avium* complex; PMN, polymorphonuclear cell; PPD, purified protein derivative; GAPDH, glyceraldehyde-3-phosphate dehydrogenase; GMM, glucose monomycolate; GPL, glycopeptidolipid; TDM, trehalose dimycolate; TLC, thin layer chromatography; TMM, trehalose monomycolate.

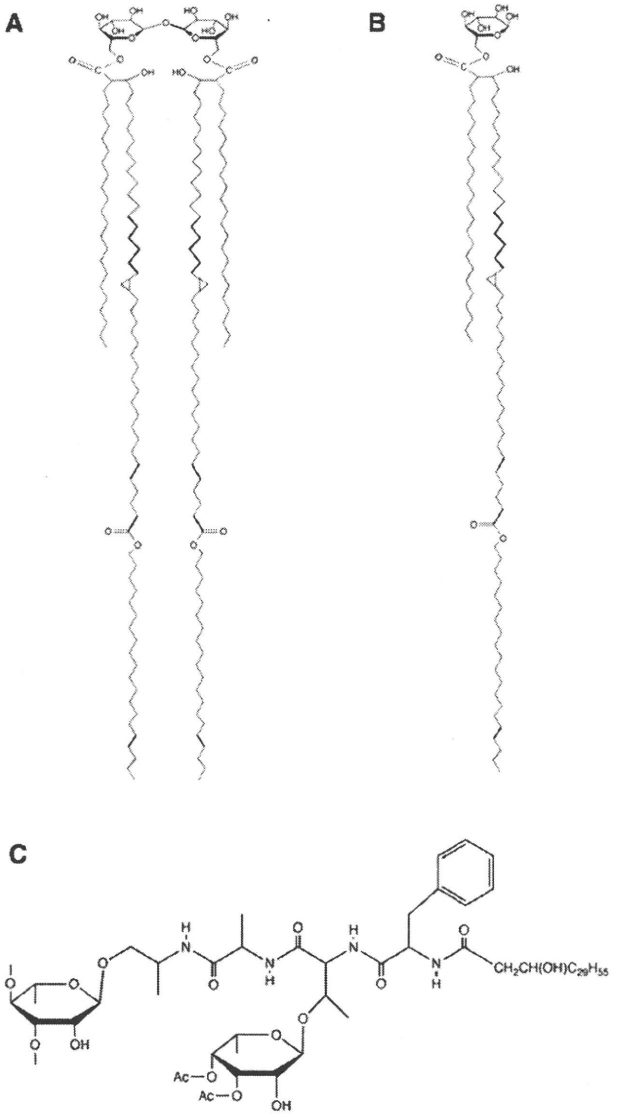

FIGURE 1. The chemical structure of TDM (*A*), GMM (*B*), and apolar GPLs (*C*).

Materials and Methods

Purification of lipid Ags from MAC and BCG

The MAC serovar 4 strain and the BCG Tokyo 172 strain were provided by Dr. Ikuya Yano (BCG Laboratory, Tokyo, Japan) and were grown at 37°C in 7H9 medium supplemented with the Middlebrook ADC enrichment (BD Biosciences). The bacteria were harvested when the OD at 600 nm reached 1–1.5. Total lipids were extracted with chloroform/methanol and separated into chloroform, acetone, and methanol fractions using open silicic acid columns as described previously (13, 14). Preparative thin layer chromatography (TLC) was further conducted to purify the major glycolipid species included in the acetone fraction, namely TDM, glucose monomycolate (GMM), and apolar glycopeptidolipids (GPLs) (Fig. 1).

TDM and GMM were extracted with chloroform/methanol (2:1, v/v) from silica gel TLC plates (Analtech) developed in chloroform/methanol/acetone/acetic acid (90:10:10:1, v/v/v/v), and the fractions were further fractionated by TLC with a solvent system of chloroform/acetone/methanol/water (50:60:2.5:3, v/v/v/v). Finally, the TDM and the GMM fractions were extracted with chloroform/methanol (2:1, v/v), dried, and rinsed with methanol. The final preparations thus obtained provided no extra spots on analytical TLC plates, and the identity of the lipids was confirmed by mass spectrometry. Protein contamination was not detected by silver staining of SDS-PAGE gels or by the Bradford assay.

The MAC serovar 4 strain-derived GPL species were resolved as closely associated spots on TLC plates due to the subtle difference in the degree of O-methylation and acetylation on sugar residues (15). Therefore, instead of purifying individual apolar GPL species, a mixture of apolar GPL species in the upper spots (upper GPL cluster) and a mixture of those in the lower spots (lower GPL cluster) were isolated from preparative TLC plates developed in chloroform/methanol (95:5, v/v).

Animals and skin tests

Four- to six-week-old female inbred strain 2 guinea pigs were purchased from Japan SLC, and housed under specific pathogen-free conditions. Either the MAC serovar 4 strain or the BCG Tokyo 172 strain was injected intradermally (1×10^8 CFU per animal), and six weeks after infection the skin area in the left flank of guinea pigs was shaved and depilated for skin tests. Indicated amounts of each lipid preparation were dissolved in 50 μl of mineral oil and were injected intradermally. Forty-eight hours after injection, the skin response was assessed by measuring the distance across the skin induration. Experiments were repeated at least twice to confirm reproducibility of the results. All animal experiments were performed according to the institutional guidelines on animal welfare and humane treatment of laboratory animals.

Histochemistry and electron microscopy

The excised skin samples were fixed for 1 day with 4% paraformaldehyde (Nacalai Tesque), dehydrated, and embedded in paraffin. The tissue sections were stained with Giemsa's stain solution (Merck), and observed under microscope. The number of eosinophils was determined in three randomly selected high power (×400) fields, and statistical analysis was performed. Separately, some skin samples were deep frozen in OCT compound, and the cryosections were labeled with mouse mAbs to guinea pig helper/inducer T cells (clone CT7) (Serotec), followed by incubation with FITC-conjugated donkey anti-mouse IgG Abs (Jackson ImmunoResearch Laboratories). After washing, the labeled sections were mounted with Vectashield mounting medium (Vector Laboratories), and viewed under fluorescence microscope. Positive cells were counted in three randomly selected high power fields.

For transmission electron microscopy, the skin was fixed with 2.5% glutaraldehyde (Polysciences), and postfixed with 2% osmium (VIII) oxide (Wako Pure Chemical). Ultrathin sections were observed under the Hitachi H-7000 electron microscope.

Cytokine mRNA expression in the Ag-challenged skin

The Ag-challenged skin was excised and the total RNA was extracted with the RNeasy mini kit (Qiagen) according to the manufacturer's instructions. The first-strand cDNA was synthesized from 0.5 μg of total RNA using oligo(dT) and PrimeScript reverse transcriptase (Takara Bio). To amplify specific transcripts, the samples were subjected to PCR amplification for 35 cycles of 30 s at 94°C, 1 min at 60°C (except for IL-5 at 63°C), 1 min at 72°C, and a final cycle of 5 min at 72°C. The primers used were: 5′-GAT ATT GTA GCC ATC AAT GAT CCC T-3′ (sense) and 5′-CAT CGT ATT TGG CCG GTT TCT CCA G-3′ (anti-sense) for glyceraldehyde-3-phosphate dehydrogenase (GAPDH); 5′-CCA TGA GCA CAG AAA GCA TGA TCC G-3′ (sense) and 5′-CTC ACA GGG CAA TGA CCC CAA AGT A-3′ (anti-sense) for TNF-α; 5′-CCA TGA GGG TGC TTC TGC AGT TGG G-3′ (sense) and 5′-CTC AGC CTT CAA TTG TCC ATT CCG T-3′ (anti-sense) for IL-5. The endpoint PCR products were resolved on 1.2% agarose gels and visualized by staining with ethidium bromide and UV transillumination. The experiments were repeated at least twice to confirm reproducibility of the results.

IL-5 mRNA expression in TDM-stimulated splenocytes

Splenocytes were isolated from either MAC-infected or mock-infected guinea pigs, and RBC were removed by treatment with the ACK lysis buffer (BioWhittaker). In some experiments, CT7-reactive cells were further removed, using the MACS MicroBeads (Miltenyi Biotec) conjugated with goat Abs to mouse IgG. The isolated cells (2×10^6 per well) were placed in wells of 24-well tissue culture plates and stimulated with 10 μg/ml TDM. For inhibition assays, either the anti-guinea pig pan group 1 CD1 mAb (clone CD1F2/6B5) (16) or an isotype-matched control mAb (clone P3) was added to the culture at the concentration of 10 μg/ml. After 16 h incubation at 37°C, the cells were harvested and the total RNA was extracted using the RNeasy mini kit (Qiagen). The first-strand cDNA synthesis and RT-PCR were conducted as described above. Each experiment was repeated at least twice to confirm reproducibility of the results.

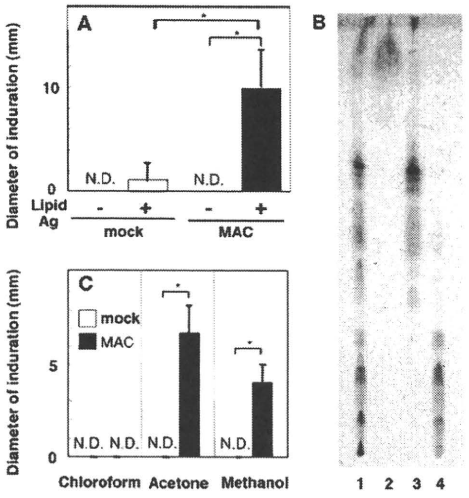

FIGURE 2. Induction of lipid-specific skin hypersensitivity in MAC-infected guinea pigs. *A*, Three mock-infected (□) and four MAC-infected (■) guinea pigs received intradermal injection of either 100 μg of the MAC-derived total lipid preparation in mineral oil (+) or mineral oil alone (−). After 48 h the diameter of the skin induration was measured (*, $p < 0.01$). *B*, The chloroform fraction (*lane 2*), the acetone fraction (*lane 3*), and the methanol fraction (*lane 4*) were obtained from the MAC-derived total lipid preparation (*lane 1*), and resolved on a TLC plate. *C*, The ability of the chloroform fraction (18 μg per animal), the acetone fraction (56 μg), and the methanol fraction (60 μg) to elicit the skin hypersensitivity in three mock-infected (□) and four MAC-infected (■) guinea pigs was assessed similarly as in *A* (*, $p < 0.01$). The dose of each fraction was determined based on its ratio of presence in the total lipid preparation. The experiments were conducted three times to confirm the reproducibility of the results. N.D., not detected.

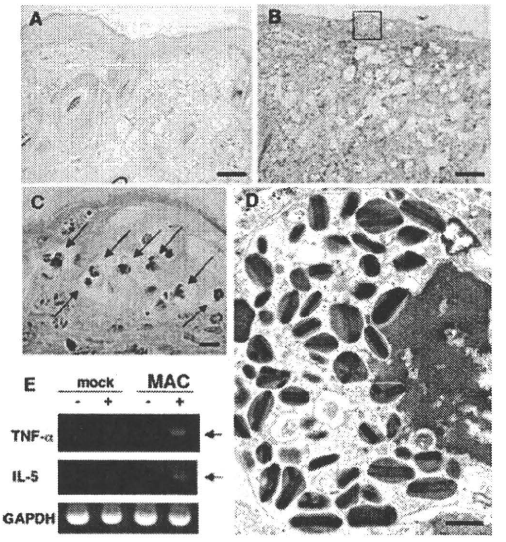

FIGURE 3. Eosinophil infiltration at the site of the glycolipid-elicited skin hypersensitivity. *A* and *B*, Mock-infected (*A*) and MAC-infected (*B*) guinea pigs received intradermal injection of the acetone fraction (56 μg per animal), and after 48 h the challenged skin specimens were subjected to Giemsa's staining. Scale bars, 100 μm. *C*, A magnified view of the boxed area in *B*. Note the infiltration of eosinophils (arrows). Scale bar, 10 μm. *D*, A transmission electron micrograph of eosinophils in the acetone fraction-challenged skin of MAC-infected guinea pigs. Scale bar, 1 μm. Note the visualization of the eosinophil-specific crystalloid core structure in cytoplasmic granules. *E*, Mock-infected and MAC-infected guinea pigs received intradermal injection of either the acetone fraction in mineral oil (+) or mineral oil alone (−). After 8 h, the challenged skin was processed for RT-PCR to detect transcripts for TNF-α, IL-5, and GAPDH. The positions of the amplified DNA for TNF-α and IL-5 on agarose gels were indicated with arrows.

Statistical analysis

Statistical analysis was performed using Student's *t* test. Values of $p < 0.05$ were considered statistically significant.

Results

Skin hypersensitivity to glycolipids in MAC-infected guinea pigs

To address whether mycobacterial lipids could elicit skin hypersensitivity in mycobacteria-infected subjects, guinea pigs were either infected with MAC or mock treated. After 6 wk these animals were subjected to the skin test with the MAC-derived total lipid preparation. None of the animals showed apparent skin changes for the first several hours. At 8 h, however, MAC-infected guinea pigs began to develop detectable induration at and around the site of intradermal injection of the total lipid preparation, with the maximum response observed at 48 h (Fig. 2*A*). Importantly, no significant skin reactions were observed in mock-infected guinea pigs challenged with the same Ag preparation, suggesting that the positive skin test required prior mycobacterial infection (Fig. 2*A*).

Fractionation of the total lipid preparation was performed to gain insights into the lipid species towards which the observed skin hypersensitivity was directed. The total lipid preparation (Fig. 2*B*, *lane 1*) was passed over open silicic acid columns to which all major lipid classes bound. The columns were then eluted sequentially with solvents of increasing polarity (chloroform, followed by acetone, and finally methanol), resulting in separation into three fractions, namely the chloroform fraction (Fig. 2*B*, *lane 2*), the acetone fraction (*lane 3*) and the methanol fraction (*lane 4*). Each fraction was then individually tested for its ability to elicit skin reactions in MAC-infected and mock-infected guinea pigs. The acetone fraction induced the most prominent skin reactions in MAC-infected, but not mock-infected, guinea pigs (Fig. 2*C*). Whereas the methanol fraction contained moderate bioactivity, no bioactivity was detected for the chloroform fraction (Fig. 2*C*). Because of its most prominent activity among the three fractions as well as the fact that it contained a majority of glycolipids, skin reactions to the acetone fraction was further characterized at molecular and cellular levels in this study.

Marked eosinophil infiltration at the site of the glycolipid-elicited skin hypersensitivity

Histochemical analysis of the skin challenged with the acetone fraction in MAC-infected guinea pigs revealed marked infiltration of polymorphonuclear (PMN) cells in the dermis (Fig. 3*B*). Infiltration of PMN cells was also detected in the epidermis, where degenerative changes or ballooning of keratinocytes were observed (Fig. 3*C*). Such changes were not detected in the skin of mock-infected guinea pigs challenged with the acetone fraction (Fig. 3*A*), confirming at the histological level that the skin hypersensitivity to the acetone fraction required prior infection. Cytoplasmic granules expressed in the infiltrating PMN cells showed eosinophilic staining with Giemsa (Fig. 3*C*, arrows) and contained electron dense crystalloid core structure (Fig. 3*D*), all of which were characteristic features of eosinophils. A small number of eosinophils and T cells appeared to begin to infiltrate around 8 h after the challenge, and there were no signs for an early wave of neutrophils (data not shown).

Among cytokines that could potentially be involved in local infiltration and accumulation of eosinophils, the cDNA sequences

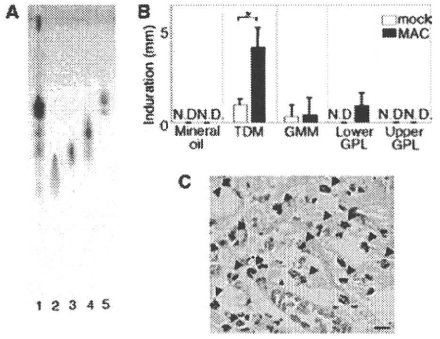

FIGURE 4. Induction of the skin hypersensitivity by TDM. *A*, TDM (*lane 2*), GMM (*lane 3*), the lower GPL cluster (*lane 4*), and the upper GPL cluster (*lane 5*) were purified from the acetone fraction (*lane 1*), followed by resolution on a TLC plate. *B*, Mock-infected (□) and MAC-infected (■) guinea pigs received intradermal injection of each lipid preparation (5 μg per animal) (*, $p < 0.05$). The hypersensitivity response at 48 h was evaluated as in Fig. 2. The experiments were conducted twice to confirm the reproducibility of the results. *C*, The specimen of the TDM-challenged skin derived from MAC-infected guinea pigs was subjected to Giemsa's staining. Note the presence of eosinophils (arrowheads) as in Fig. 3. Scale bar, 10 μm. N.D., not detected.

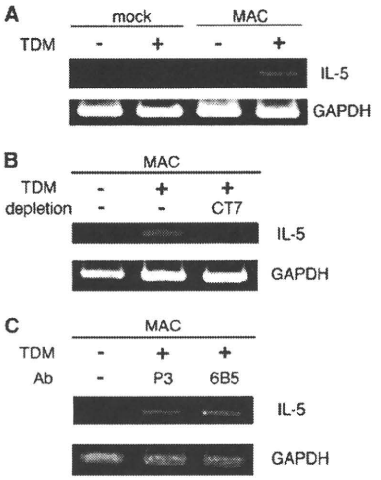

FIGURE 5. In vitro response of MAC-infected guinea pig-derived splenocytes to TDM. *A*, Splenocytes were isolated from either MAC-infected or mock-infected guinea pigs and cultured for 16 h in the presence or absence of TDM. The cells were then harvested and the total RNA was extracted, followed by RT-PCR to detect IL-5 and GAPDH transcription. Note that MAC-infected, but not mock-infected, guinea pig-derived splenocytes up-regulated IL-5 transcription by stimulation with TDM. *B*, Splenocytes before and after depletion of CT7-reactive cells were stimulated with TDM, and RT-PCR was performed as in *A*. Note that removal of $CT7^+$ T cells resulted in the loss of IL-5 transcription. *C*, MAC-infected guinea pig-derived splenocytes were stimulated with TDM either in the presence of saturating amounts of anti-guinea pig pan group 1 CD1 mAb (clone CD1F2/6B5) or an isotype-matched control mAb (clone P3), and RT-PCR was performed as in *A*. The TDM-elicited IL-5 transcription was observed similarly in both conditions.

for guinea pig TNF-α and IL-5 have already been published, enabling us to assess their local expression by RT-PCR. Eight hours after intradermal injection of either the acetone fraction in mineral oil or mineral oil alone, the skin specimens were obtained and the total RNA was extracted, followed by RT-PCR with specific primers. As shown in Fig. 3*E*, expression of TNF-α and IL-5 was up-regulated only in the acetone fraction-challenged skin of MAC-infected guinea pigs. Because both TNF-α and IL-5 are known to facilitate recruitment of eosinophils to the inflammatory foci of tissues (17), specific induction of these cytokines in the acetone fraction-challenged skin of MAC-infected animals would likely support local infiltration and accumulation of eosinophils.

Identification of TDM as a glycolipid species eliciting the eosinophilic skin hypersensitivity

To determine the lipid species in the acetone fraction capable of eliciting the eosinophilic skin hypersensitivity, major lipid species contained in the acetone fraction, namely TDM (Fig. 4*A*, *lane 2*), GMM (*lane 3*), upper GPL clusters (*lane 4*), and lower GPL clusters (*lane 5*) were purified from the acetone fraction (*lane 1*) as described in *Materials and Methods*, and tested individually for their bioactivity. As shown in Fig. 4*B*, significant skin reactions were elicited only in MAC-infected guinea pigs challenged with TDM, but not with other glycolipid preparations including GMM, a known CD1-presented mycolyl glycolipid (18, 19). Histochemical analysis of the TDM-challenged skin in infected animals detected prominent infiltration of eosinophils (Fig. 4*C*, arrowheads), as seen in the skin challenged with the acetone fraction (Fig. 3, *B* and *C*). The number of infiltrating eosinophils in response to TDM was significantly higher in MAC-infected guinea pigs (137 ± 26.6 cells/field, $p < 0.01$) than in uninfected animals (7.2 ± 12.5 cells/field).

TDM-induced IL-5 induction by splenocytes derived from MAC-infected guinea pigs

As shown above, the TDM-induced, eosinophilic skin reaction was observed only in MAC-infected guinea pigs, suggesting the possibility that MAC infection might prime immune cells to respond by IL-5 secretion upon subsequent challenge with TDM. Indeed, when splenocytes derived from MAC-infected or mock-infected guinea pigs were stimulated in vitro with TDM, only those derived from MAC-infected guinea pigs up-regulated IL-5 mRNA expression in response to TDM (Fig. 5*A*). Depletion of guinea pig "helper/inducer" T cells, defined by reactivity to the CT7 mAb, completely abrogated the IL-5 mRNA induction (Fig. 5*B*). Considering the mycolic acid-containing glycolipid structure of TDM that was shared with the CD1-presented GMM Ag, we addressed whether the TDM-elicited IL-5 induction by CT7-reactive T cells might depend on CD1 function. As shown in Fig. 5*C*, TDM-stimulated splenocytes up-regulated IL-5 mRNA expression even in the presence of saturating amounts of an anti-pan group 1 CD1 mAb (6B5), suggesting the possibility that the TDM-elicited, eosinophilic skin hypersensitivity might not depend on the function of the known guinea pig group 1 CD1 molecules.

The TDM-specific skin reaction was distinct from the classical DTH reaction to protein Ags

TDM is expressed in all mycobacteria species so far analyzed (20). To address whether the TDM-specific hypersensitivity reaction induced in MAC-infected guinea pigs might be observed also in guinea pigs infected with other mycobacteria species, and to directly compare the response with the classical DTH reactions against PPD (the tuberculin test), guinea pigs were immunized with BCG, and histochemical analysis of the skin challenged with either mineral oil alone, *M. tuberculosis*-derived PPD, or BCG-derived TDM was performed in parallel. Although infiltrating cells were not apparent in the mock-challenged skin (Fig. 6*A*), significant infiltration of mononuclear cells was observed in the PPD-challenged skin (Fig. 6, *B* and *E*), in which few eosinophils were detected (Fig. 6*D*). In sharp contrast, eosinophil infiltration was prominent in the TDM-challenged skin (Fig. 6, *C* and *D*), as seen

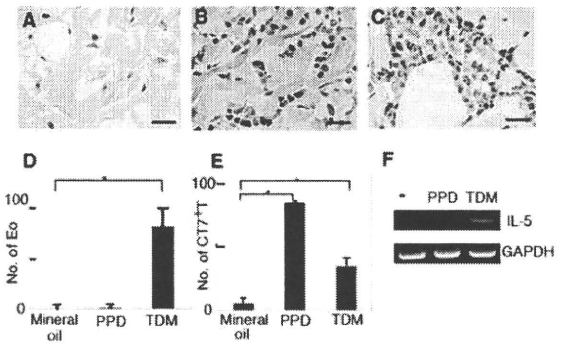

FIGURE 6. TDM-elicited eosinophilic skin hypersensitivity was distinct from the classical DTH to protein Ags in BCG-immunized guinea pigs. *A–C*, BCG-immunized guinea pigs received intradermal injection of either mineral oil (*A*), 0.5 μg of PPD (*B*), or 20 μg of BCG-derived TDM (*C*), and specimens of the Ag-challenged skin were subjected to Giemsa's staining. Scale bars, 50 μm. *D* and *E*, The average number of infiltrating eosinophils (*D*) and $CD7^+$ T cells (*E*) per high power field (×400) was determined for each of the three groups. (*, $p < 0.01$). *F*, Total RNA was extracted from the mock-, PPD-, and TDM-challenged skin, and in situ transcription of IL-5 and GAPDH was determined by RT-PCR. Note that IL-5 transcription was detected only in TDM-challenged skin, but not in PPD-challenged skin.

in MAC-infected guinea pigs (Fig. 4). Furthermore, in situ up-regulation of IL-5 mRNA expression was observed only in the TDM-challenged skin, but not in PPD-challenged skin (Fig. 6*F*). Taken together, the results obtained in the present study indicated that the TDM-induced response define a form of skin hypersensitivity that required prior mycobacterial infection but was distinct from the classical DTH reaction to protein Ags.

Discussion

We and others (10, 21, 22) have previously detected mycobacteria-specific, group 1 CD1-restricted T responses in humans in a form analogous to that of a classical Th1 memory response to protein Ags. Therefore, the present study was initially intended to determine whether CD1-presented glycolipid Ags, such as GMM, might elicit DTH responses that were comparable to those directed against protein Ags. Similar to the classical DTH response, the TDM-elicited skin hypersensitivity identified in this study required prior mycobacterial infection, and the peak response was observed 48 h after the Ag challenge (Figs. 2 and 4). Further, specific Abs to TDM were not detected in the sera of infected guinea pigs, and administration of the sera and TDM to the skin of naive guinea pigs did not elicit any significant responses (data not shown), making it unlikely that the TDM-elicited skin response was a persistent form of immediate hypersensitivity or type I immunity. Notably, the TDM-elicited skin hypersensitivity involved prominent infiltration of eosinophils and up-regulation of IL-5 transcription, sharply contrasting with the PPD-elicited skin hypersensitivity (Fig. 6). Thus, the TDM-elicited skin response apparently defines a form of hypersensitivity that is distinct from the classical Th1-dominant DTH response to protein Ags. The identity of the TDM-specific memory T cell response detected in the spleen of mycobacteria-infected guinea pigs has not been fully determined, primarily due to the paucity of useful reagents for guinea pig studies. Interestingly, the TDM-elicited eosinophilic hypersensitivity was not induced in mice (data not shown), underscoring that the use of the guinea pig model is more appropriate. This may also suggest that immune elements, such as group 1 CD1 molecules, that exist in guinea pigs but not in mice could mediate the response. However, the blocking experiments with specific Abs indicated that none of the seven guinea pig group 1 CD1 molecules, namely four homologues of human CD1b and three homologues of human CD1c (16, 23), might not be involved directly in the TDM-elicited T cell activation (Fig. 5). Besides T cells of the adaptive immunity, those that function in the interphase between innate and adaptive immunity, such as group 2 CD1 (CD1d)-reactive NKT cells, may be relevant to the guinea pig model of the TDM-elicited hypersensitivity. TDM-induced granulomatous responses have been shown to be impaired in mice in the absence of CD1d function (24), suggesting a role for NKT cells in hypersensitive responses in mycobacterial infection. Further, a prolonged expansion of NKT cells has been noted during mycobacterial infection (25), possibly by recognition of mycobacterial phosphatidylinositol mannosides (26). A subsequent challenge with TDM may induce TLR-dependent up-regulation of IL-15 expression in $CD1d^+$ macrophages (27), resulting in activation of a unique subset of group 2 CD1 (CD1d)-reactive NKT cells which has been shown to secrete IL-5 in the presence of $CD1d^+$ APCs and IL-15 (28). So far, guinea pig *CD1D* genes have not been identified (23), but conservation of the genes across mammalian species suggests that NKT cells may also exist in guinea pigs. Alternatively, it is still possible that CD1-unrestricted T cell subsets that include $\gamma\delta$ T cells may also contribute to the eosinophilic skin response.

The infiltration of eosinophils at the site of infection has been observed in human cases with tuberculosis (29–32) and in animals infected with either *M. tuberculosis*, *M. bovis*, or *M. avium* (33–36), but microbial components that trigger the eosinophilic response were unclear. The present study indicates that TDM and some other undefined lipid components, possibly trehalose monomycolate (TMM), in the methanol fraction (Fig. 2*C*) are potent in triggering the eosinophilic response. Immune recognition of mycobacterial TDM followed by eosinophilic inflammation may function as a component of host defense because of the anti-mycobacterial effect of eosinophil peroxidase present at high levels in specific granules of eosinophils (37). The TDM-elicited eosinophilic response may highlight a new aspect of protective and pathological processes involved in mycobacterial infection.

This also raises an issue of how mycobacteria suppress or escape from the noxious attack from the host eosinophils. We recently found that mycobacteria could reduce the expression of TDM soon after their entry into the host by borrowing host-derived glucose to replace TDM with GMM. Mycobacterial mycolyltransferases are known to catalyze the final step of TDM synthesis from its precursor, TMM, by addition of a mycolyl acyl group. Upon exposure to host-derived glucose, however, competitive substrate selection of TMM and glucose by mycolyltransferases results in down-regulation of TDM accompanied with up-regulated biosynthesis of GMM (38). As shown in Fig. 4*B*, GMM is inefficient in eliciting the eosinophilic response, and thus the mycolyltransferase-mediated glycolipid exchange may be an evasive maneuver that mycobacteria have evolved to avoid the eosinophilic host response. It is now intriguing to propose that GMM-specific, CD1-restricted T cell responses, detected in human cases with mycobacterial infection (10, 18, 19), come into play to control these GMM-rich mycobacteria. Cell wall mycolyl glycolipids have often proved critical for survival and virulence of mycobacteria (11). The present study suggests that host defense mechanisms directed against these critical glycolipid components can be activated at different stages of immunity, providing the host with an opportunity to efficiently monitor and control infection with mycobacteria.

Acknowledgments

We thank Dr. Chris C. Dascher (Mount Sinai School of Medicine, New York, NY) for the critical reading of the manuscript. We also thank Dr.

Ikuya Yano (BCG laboratory, Tokyo, Japan) for providing valuable materials.

Disclosures

The authors have no financial conflict of interest.

References

1. Chaicumpar, K., N. Fujiwara, O. Nishimura, H. Hotta, J. W. Pan, M. Takahashi, C. Abe, and I. Yano. 1997. Studies of polymorphic DNA fingerprinting and lipid pattern of *Mycobacterium tuberculosis* patient isolates in Japan. *Microbiol. Immunol.* 41: 107–119.
2. Kobayashi, K., K. Kaneda, and T. Kasama. 2001. Immunopathogenesis of delayed-type hypersensitivity. *Microsc. Res. Tech.* 53: 241–245.
3. Orme, I. M., and A. M. Cooper. 1999. Cytokine/chemokine cascades in immunity to tuberculosis. *Immunol. Today* 20: 307–312.
4. Chackerian, A. A., T. V. Perera, and S. M. Behar. 2001. γ interferon-producing $CD4^+$ T lymphocytes in the lung correlate with resistance to infection with *Mycobacterium tuberculosis*. *Infect. Immun.* 69: 2666–2674.
5. Ulrichs, T., and S. H. Kaufmann. 2006. New insights into the function of granulomas in human tuberculosis. *J. Pathol.* 208: 261–269.
6. Casanova, J. L., and L. Abel. 2002. Genetic dissection of immunity to mycobacteria: the human model. *Annu. Rev. Immunol.* 20: 581–620.
7. Salgame, P. 2005. Host innate and Th1 responses and the bacterial factors that control *Mycobacterium tuberculosis* infection. *Curr. Opin. Immunol.* 17: 374–380.
8. Behar, S. M., and S. A. Porcelli. 2007. CD1-restricted T cells in host defense to infectious diseases. *Curr. Topics Microbiol. Immunol.* 314: 215–250.
9. Moody, D. B., T. Ulrichs, W. Muhlecker, D. C. Young, S. S. Gurcha, E. Grant, J. P. Rosat, M. B. Brenner, C. E. Costello, G. S. Besra, and S. A. Porcelli. 2000. CD1c-mediated T-cell recognition of isoprenoid glycolipids in *Mycobacterium tuberculosis* infection. *Nature* 404: 884–888.
10. Ulrichs, T., D. B. Moody, E. Grant, S. H. Kaufmann, and S. A. Porcelli. 2003. T-cell responses to CD1-presented lipid antigens in humans with *Mycobacterium tuberculosis* infection. *Infect. Immun.* 71: 3076–3087.
11. Rao, V., N. Fujiwara, S. A. Porcelli, and M. S. Glickman. 2005. *Mycobacterium tuberculosis* controls host innate immune activation through cyclopropane modification of a glycolipid effector molecule. *J. Exp. Med.* 201: 535–543.
12. Dascher, C. C., K. Hiromatsu, X. Xiong, C. Morehouse, G. Watts, G. Liu, D. N. McMurray, K. P. LeClair, S. A. Porcelli, and M. B. Brenner. 2003. Immunization with a mycobacterial lipid vaccine improves pulmonary pathology in the guinea pig model of tuberculosis. *Int. Immunol.* 15: 915–925.
13. Hiromatsu, K., C. C. Dascher, K. P. LeClair, M. Sugita, S. T. Furlong, M. B. Brenner, and S. A. Porcelli. 2002. Induction of CD1-restricted immune responses in guinea pigs by immunization with mycobacterial lipid antigens. *J. Immunol.* 169: 330–339.
14. Matsunaga, I., A. Bhatt, D. C. Young, T. Y. Cheng, S. J. Eyles, G. S. Besra, V. Briken, S. A. Porcelli, C. E. Costello, W. R. Jacobs, Jr., and D. B. Moody. 2004. *Mycobacterium tuberculosis* pks12 produces a novel polyketide presented by CD1c to T cells. *J. Exp. Med.* 200: 1559–1569.
15. Chatterjee, D., and K. H. Khoo. 2001. The surface glycopeptidolipids of mycobacteria: structures and biological properties. *Cell Mol. Life Sci.* 58: 2018–2042.
16. Hiromatsu, K., C. C. Dascher, M. Sugita, C. Gingrich-Baker, S. M. Behar, K. P. LeClair, M. B. Brenner, and S. A. Porcelli. 2002. Characterization of guinea-pig group 1 CD1 proteins. *Immunology* 106: 159–172.
17. Lampinen, M., M. Carlson, L. D. Hakansson, and P. Venge. 2004. Cytokine-regulated accumulation of eosinophils in inflammatory disease. *Allergy* 59: 793–805.
18. Moody, D. B., M. R. Guy, E. Grant, T. Y. Cheng, M. B. Brenner, G. S. Besra, and S. A. Porcelli. 2000. CD1b-mediated T cell recognition of a glycolipid antigen generated from mycobacterial lipid and host carbohydrate during infection. *J. Exp. Med.* 192: 965–976.
19. Moody, D. B., B. B. Reinhold, M. R. Guy, E. M. Beckman, D. E. Frederique, S. T. Furlong, S. Ye, V. N. Reinhold, P. A. Sieling, R. L. Modlin, et al. 1997. Structural requirements for glycolipid antigen recognition by CD1b- restricted T cells. *Science* 278: 283–286.
20. Ryll, R., Y. Kumazawa, and I. Yano. 2001. Immunological properties of trehalose dimycolate (cord factor) and other mycolic acid-containing glycolipids: a review. *Microbiol. Immunol.* 45: 801–811.
21. Kawashima, T., Y. Norose, Y. Watanabe, Y. Enomoto, H. Narazaki, E. Watari, S. Tanaka, H. Takahashi, I. Yano, M. B. Brenner, and M. Sugita. 2003. Cutting edge: major CD8 T cell response to live bacillus Calmette-Guerin is mediated by CD1 molecules. *J. Immunol.* 170: 5345–5348.
22. Watanabe, Y., E. Watari, I. Matsunaga, K. Hiromatsu, C. C. Dascher, T. Kawashima, Y. Norose, K. Shimizu, H. Takahashi, I. Yano, and M. Sugita. 2006. BCG vaccine elicits both T-cell mediated and humoral immune responses directed against mycobacterial lipid components. *Vaccine* 24: 5700–5707.
23. Dascher, C. C., K. Hiromatsu, J. W. Naylor, P. P. Brauer, K. A. Brown, J. R. Storey, S. M. Behar, E. S. Kawasaki, S. A. Porcelli, M. B. Brenner, and K. P. LeClair. 1999. Conservation of a CD1 multigene family in the guinea pig. *J. Immunol.* 163: 5478–5488.
24. Guidry, T. V., R. L. Hunter, Jr., and J. K. Actor. 2006. $CD3^+$ cells transfer the hypersensitive granulomatous response to mycobacterial glycolipid trehalose 6,6′-dimycolate in mice. *Microbiology* 152: 3765–3775.
25. Dieli, F., M. Taniguchi, M. Kronenberg, S. Sidobre, J. Ivanyi, L. Fattorini, E. Iona, G. Orefici, G. De Leo, D. Russo, et al. 2003. An anti-inflammatory role for V α14 NK T cells in *Mycobacterium bovis* bacillus Calmette-Guerin-infected mice. *J. Immunol.* 171: 1961–1968.
26. Fischer, K., E. Scotet, M. Niemeyer, H. Koebernick, J. Zerrahn, S. Maillet, R. Hurwitz, M. Kursar, M. Bonneville, S. H. Kaufmann, and U. E. Schaible. 2004. Mycobacterial phosphatidylinositol mannoside is a natural antigen for CD1d-restricted T cells. *Proc. Natl. Acad. Sci. USA* 101: 10685–10690.
27. Krutzik, S. R., B. Tan, H. Li, M. T. Ochoa, P. T. Liu, S. E. Sharfstein, T. G. Graeber, P. A. Sieling, Y. J. Liu, T. H. Rea, et al. 2005. TLR activation triggers the rapid differentiation of monocytes into macrophages and dendritic cells. *Nat. Med.* 11: 653–660.
28. Sakuishi, K., S. Oki, M. Araki, S. A. Porcelli, S. Miyake, and T. Yamamura. 2007. Invariant NKT cells biased for IL-5 production act as crucial regulators of inflammation. *J. Immunol.* 179: 3452–3462.
29. Flores, M., J. Merino-Angulo, J. G. Tanago, and C. Aquirre. 1983. Late generalized tuberculosis and eosinophilia. *Arch. Intern. Med.* 143: 182.
30. Nathan, N., N. Guillemot, G. Aubertin, S. Blanchon, K. Chadelat, R. Epaud, A. Clement, and B. Fauroux. 2008. Chronic eosinophilic pneumonia in a 13-year-old child. *Eur. J. Pediatr.* 167: 1203–1207.
31. Ozaki, T., S. Nakahira, K. Tani, F. Ogushi, S. Yasuoka, and T. Ogura. 1992. Differential cell analysis in bronchoalveolar lavage fluid from pulmonary lesions of patients with tuberculosis. *Chest* 102: 54–59.
32. Vijayan, V. K., A. M. Reetha, M. S. Jawahar, K. Sankaran, and R. Prabhakar. 1992. Pulmonary eosinophilia in pulmonary tuberculosis. *Chest* 101: 1708–1709.
33. Castro, A. G., N. Esaguy, P. M. Macedo, A. P. Aguas, and M. T. Silva. 1991. Live but not heat-killed mycobacteria cause rapid chemotaxis of large numbers of eosinophils in vivo and are ingested by the attracted granulocytes. *Infect. Immun.* 59: 3009–3014.
34. D'Avila, H., P. E. Almeida, N. R. Roque, H. C. Castro-Faria-Neto, and P. T. Bozza. 2007. Toll-like receptor-2-mediated C-C chemokine receptor 3 and eotaxin-driven eosinophil influx induced by *Mycobacterium bovis* BCG pleurisy. *Infect. Immun.* 75: 1507–1511.
35. Lasco, T. M., O. C. Turner, L. Cassone, I. Sugawara, H. Yamada, D. N. McMurray, and I. M. Orme. 2004. Rapid accumulation of eosinophils in lung lesions in guinea pigs infected with *Mycobacterium tuberculosis*. *Infect. Immun.* 72: 1147–1149.
36. Ordway, D., G. Palanisamy, M. Henao-Tamayo, E. E. Smith, C. Shanley, I. M. Orme, and R. J. Basaraba. 2007. The cellular immune response to *Mycobacterium tuberculosis* infection in the guinea pig. *J. Immunol.* 179: 2532–2541.
37. Borelli, V., F. Vita, S. Shankar, M. R. Soranzo, E. Banfi, G. Scialino, C. Brochetta, and G. Zabucchi. 2003. Human eosinophil peroxidase induces surface alteration, killing, and lysis of *Mycobacterium tuberculosis*. *Infect. Immun.* 71: 605–613.
38. Matsunaga, I., T. Naka, R. S. Talekar, M. J. McConnell, K. Katoh, H. Nakao, A. Otsuka, S. M. Behar, I. Yano, D. B. Moody, and M. Sugita. 2008. Mycolyltransferase-mediated glycolipid exchange in mycobacteria. *J. Biol. Chem.* 283: 28835–28841.

JOURNAL OF BACTERIOLOGY, Dec. 2008, p. 7918–7924 Vol. 190, No. 24
0021-9193/08/$08.00+0 doi:10.1128/JB.00911-08

The *Mycobacterium avium* Complex *gtfTB* Gene Encodes a Glucosyltransferase Required for the Biosynthesis of Serovar 8-Specific Glycopeptidolipid[▽]

Yuji Miyamoto,[1]* Tetsu Mukai,[1] Yumi Maeda,[1] Masanori Kai,[1] Takashi Naka,[2] Ikuya Yano,[2] and Masahiko Makino[1]

Department of Microbiology, Leprosy Research Center, National Institute of Infectious Diseases, 4-2-1 Aobacho, Higashimurayama, Tokyo 189-0002, Japan,[1] and Japan BCG Central Laboratory, 3-1-5 Matsuyama, Kiyose, Tokyo 204-0022, Japan[2]

Received 2 July 2008/Accepted 29 September 2008

***Mycobacterium avium* complex (MAC) is one of the most common opportunistic pathogens widely distributed in the natural environment. The 28 serovars of MAC are defined by variable oligosaccharide portions of glycopeptidolipids (GPLs) that are abundant on the surface of the cell envelope. These GPLs are also known to contribute to the virulence of MAC. Serovar 8 is one of the dominant serovars isolated from AIDS patients, but the biosynthesis of serovar 8-specific GPL remains unknown. To clarify this, we compared gene clusters involved in the biosynthesis of several serovar-specific GPLs and identified the genomic region predicted to be responsible for GPL biosynthesis in a serovar 8 strain. Sequencing of this region revealed the presence of four open reading frames, three unnamed genes and *gtfTB*, the function of which has not been elucidated. The simultaneous expression of *gtfTB* and two downstream genes in a recombinant *Mycobacterium smegmatis* strain genetically modified to produce serovar 1-specific GPL resulted in the appearance of 4,6-*O*-(1-carboxyethylidene)-3-*O*-methyl-glucose, which is unique to serovar 8-specific GPL, suggesting that these three genes participate in its biosynthesis. Furthermore, functional analyses of *gtfTB* indicated that it encodes a glucosyltransferase that transfers a glucose residue via 1→3 linkage to a rhamnose residue of serovar 1-specific GPL, which is critical to the formation of the oligosaccharide portion of serovar 8-specific GPL. Our findings might provide a clue to understanding the biosynthetic regulation that modulates the biological functions of GPLs in MAC.**

Mycobacteria are pathogens that cause diseases such as tuberculosis and leprosy. In addition, nontuberculous mycobacteria, which are widely distributed in the natural environment, cause opportunistic pulmonary infections resembling tuberculosis. These mycobacteria are distinguished by a multilayered cell envelope consisting of peptidoglycan, mycolyl arabinogalactan, and surface glycolipids (9, 13). The surface glycolipids are abundant and structurally different, and they may act as a barrier to immune responses (9, 13). Glycopeptidolipids (GPLs) are major glycolipid components present on the surface of several species of nontuberculous mycobacteria (40). All of these GPLs have a conserved core structure that is composed of a fatty acyl tetrapeptide glycosylated with 6-deoxytalose (6-d-Tal) and *O*-methyl-rhamnose (O-Me-Rha) and are termed non-serovar-specific GPLs (nsGPLs) (2, 4, 14). On the other hand, the GPLs of *Mycobacterium avium* complex (MAC), nontuberculous mycobacteria consisting principally of two species, *M. avium* and *M. intracellulare*, have various haptenic oligosaccharides linked to the 6-d-Tal residue of nsGPLs, resulting in serovar-specific GPLs (ssGPLs) (2, 4, 40). The oligosaccharide portions of ssGPLs define MAC serovars that are classified into 28 types. The serovar 1-specific GPL, with Rha linked to the 6-d-Tal residue, is the basic oligosaccharide unit of all ssGPLs (11). The Rha residue of serovar 1-specific GPL is further extended by various glycosylation steps, such as rhamnosylation, fucosylation, and glucosylation (11). These glycosylation steps generate structural diversity in GPLs of MAC (11). However, because of their complexity, most of the biosynthetic pathways for ssGPLs have not been fully determined. We recently showed that the biosynthesis of nsGPLs was regulated by a combination of glycosyltransferases (31). Therefore, each glycosyltransferase might mediate a specific step in the biosynthesis of ssGPLs.

In terms of biological activity, it has been reported that the properties of ssGPLs are notably different from each other and that some of the properties play a role in affecting host responses to MAC infections (3, 5, 21, 27, 37, 38). Moreover, epidemiological studies have shown that serovars 1, 4, and 8 are distributed predominantly in North America and are also frequently isolated from AIDS patients (24, 39, 41). However, in contrast to other ssGPLs, the serovar 8-specific GPL is reported to be able to induce altered immune responses (3, 21). The biosynthetic pathway for serovar 8-specific GPL, particularly its oligosaccharide portion that includes a unique 4,6-*O*-(1-carboxyethylidene)-3-*O*-methyl-glucose (Glc) residue (7, 8) that may determine the specificity of serovar 8, remains unknown (Table 1). In this study, we investigated the genomic region assumed to be associated with the biosynthesis of GPL in MAC serovar 8 strain and identified the genes involved in

* Corresponding author. Mailing address: Department of Microbiology, Leprosy Research Center, National Institute of Infectious Diseases, 4-2-1 Aobacho, Higashimurayama, Tokyo 189-0002, Japan. Phone: 81-42-391-8211. Fax: 81-42-394-9092. E-mail: yujim@nih.go.jp.

▽ Published ahead of print on 10 October 2008.

TABLE 1. Oligosaccharide structures of serovar 1- and 8-specific GPLs

Serovar	Oligosaccharide	Reference(s)
1	α-L-Rha-(1→2)-L-6-d-Tal	17
8	4,6-*O*-(1-carboxyethylidene)-3-*O*-methyl-β-D-Glc-(1→3)-α-L-Rha-(1→2)-L-6-d-Tal	7, 8

the glycosylation pathway leading to the formation of serovar 8-specific GPL.

MATERIALS AND METHODS

Bacterial strains, culture conditions, and DNA manipulation. Table 2 shows the bacterial strains and vectors used in this study. MAC strains were grown in Middlebrook 7H9 broth (Difco) with 0.05% Tween 80 supplemented with 10% Middlebrook ADC enrichment (BBL). Recombinant *M. smegmatis* strains used for GPL production were cultured in Luria-Bertani broth with 0.2% Tween 80. Isolation of DNA and transformation of *M. smegmatis* strains were performed as previously described (32). The genomic regions of MAC strains were amplified by a two-step PCR using TaKaRa *LA Taq* with GC buffer and the following program: denaturation at 98°C for 20 s and annealing-extension at 68°C for an appropriate time depending on the length of the targeted region. *Escherichia coli* strain DH5α was used for routine manipulation and propagation of plasmid DNA. When necessary, antibiotics were added as follows: kanamycin, 50 μg/ml for *E. coli* and 25 μg/ml for *M. smegmatis*; and hygromycin B, 150 μg/ml for *E. coli* and 75 μg/ml for *M. smegmatis*. Oligonucleotide primers used in this study are listed in Table 3.

Construction of expression vectors. The *rtfA* gene was amplified from genomic DNA of *M. avium* strain JATA51-01 using primers RTFA-S and RTFA-A. The PCR products were digested with each restriction enzyme and cloned into the BamHI-PstI site of pMV261 to obtain pMV-rtfA. To use the site-specific integrating mycobacterial vector more conveniently, we constructed pYM301a containing an AflII site in pYM301. The region encompassing *gtfTB*, ORF3, and ORF4 was amplified from genomic DNA of MAC serovar 8 strain ATCC 35771 using primers GTFTB-S and ORF4-A. In addition, *gtfTB* was amplified using primers GTFTB-S and GTFTB-A. The PCR products were digested with each restriction enzyme and cloned into the PstI-EcoRI site of pYM301a to obtain pYM-gtfTB-orf3-orf4 and pYM-gtfTB (Table 2).

Isolation and purification of GPLs. Harvested bacterial cells were allowed to stand in $CHCl_3$-CH_3OH (2:1, vol/vol) for several hours at room temperature. After water was added, total-lipid extracts were obtained from the organic phase and evaporated to dryness. Total-lipid extracts were subjected to mild alkaline hydrolysis as previously described (32, 33) to obtain crude GPL extracts. For analytical thin-layer chromatography (TLC), crude GPLs obtained from the same wet weight of harvested bacterial cells were spotted on Silica Gel 60 plates (Merck) using $CHCl_3$-CH_3OH-H_2O (30:8:1, vol/vol/vol) as the solvent and were visualized by spraying the plates with 10% H_2SO_4 and charring. Purified GPLs were prepared from crude GPLs by preparative TLC on the same plates, and each GPL was extracted from the corresponding band. Perdeuteriomethylation was carried out as previously described (6, 12, 17).

TABLE 3. Oligonucleotide primers used in this study

Primer	Sequence[a]	Restriction site
RTFA-S	5′-CGGGATCCCATGAAATTTGCTGTGGCAAG-3′	BamHI
RTFA-A	5′-AACTGCAGCTCAGCGACTTCGCTGCGCTTC-3′	PstI
GTFTB-S	5′-AACTGCAGAAATGACCGCCACAACCAGGGC-3′	PstI
GTFTB-A	5′-GGAATTCTCAGGCGCTCAGTGGCTCGTC-3′	EcoRI
ORF4-A	5′-GGAATTCCTAGGGCGCCAATTCGATGAG-3′	EcoRI
GTFB-U4	5′-GGAATTCGGTCGACTCGACGAAGCCGAC-3′	EcoRI
DRRC-A	5′-GGAATTCTGCAGGCGGGGCGACTCCTGCT-3′	EcoRI

[a] Underlining indicates restriction sites.

GC-MS and MALDI-TOF MS analysis. Crude and purified GPLs were hydrolyzed in 2 M trifluoroacetic acid (2 h, 120°C), and the released sugars were reduced with $NaBD_4$ and then acetylated with pyridine-acetic anhydride (1:1, vol/vol) at room temperature overnight. The resulting alditol acetates were separated and analyzed by gas chromatography-mass spectrometry (GC-MS) with a TRACE DSQ (Thermo Electron) equipped with an SP-2380 column (Supelco) using helium gas. The following program was used: temperature increased from 52 to 172°C at a rate of 40°C/min and then increased from 172 to 250°C at a rate of 3°C/min. To determine the total mass of the purified GPLs, matrix-assisted laser desorption ionization—time of flight (MALDI-TOF) mass spectra (in the positive mode) were obtained with a QSTAR XL (Applied Biosystems) using a pulse laser with emission at 337 nm. Samples mixed with 2,5-dihydroxybenzoic acid as the matrix were analyzed in the reflectron mode with an accelerating voltage of 20 kV and with operation in positive ion mode.

Nucleotide sequence accession number. The 4.6-kb genomic region amplified from MAC serovar 8 strain ATCC 35771 using primers GTFB-U4 and DRRC-A has been deposited in the DDBJ nucleotide sequence database under accession number AB437139.

RESULTS

Isolation and sequencing of the 4.6-kb genomic region responsible for GPL biosynthesis in MAC serovar 8. Lacking information on the genes responsible for biosynthesis of serovar 8-specific GPL, we compared and analyzed the genomic regions likely to be responsible for GPL biosynthesis in several

TABLE 2. Bacterial strains and vectors used in this study

Strain or vector	Characteristics	Source or reference
Bacteria		
E. coli DH5α	Cloning host	TaKaRa
M. smegmatis mc^{2}155	Expression host	35
M. intracellulare ATCC 35771	MAC serovar 8 strain	29
M. avium JATA51-01	Source of *rtfA*	17
Vectors		
pYM301	Source of pYM301a	30
pYM301a	Site-specific integrating mycobacterial vector carrying an *hsp60* promoter cassette and AflII site	This study
pMV261	*E. coli-Mycobacterium* shuttle vector carrying an *hsp60* promoter cassette	36
pMV-rtfA	pMV261 with *rtfA*	This study
pYM-gtfTB	pYM301a with *gtfTB*	This study
pYM-gtfTB-orf3-orf4	pYM301a with *gtfTB*, ORF3, and ORF4	This study

FIG. 1. Organization of the 4.6-kb genomic region isolated from MAC serovar 8 strain. Filled triangles indicate the primers used for PCR amplification.

MAC serovars (16, 28). Most of these regions have high homology to each other, while the segment between the *gtfB* and *drrC* genes was found to vary in the strains. Therefore, we assumed that this segment contains genes involved in the formation of the unique Glc residue in serovar 8-specific GPL. To clone the *gtfB-drrC* region by using PCR, we designed various primers containing sequences derived from other MAC strains. By examining combinations of several pairs of primers, a 4.6-kb fragment was amplified from genomic DNA of a MAC serovar 8 strain when primers GTFB-U4 and DRRC-A were used (Fig. 1). Sequencing of this 4.6-kb fragment revealed four complete open reading frames (Fig. 1). The deduced amino acid sequences encoded by ORF1, ORF2, ORF3, and ORF4 were found to be identical to the amino acid sequences of four functionally undefined proteins from *M. avium* strain 104, MAV_3253, MAV_3255, MAV_3256, and MAV_3257, respectively (GenBank accession no. NC_008595.1). *M. avium* strain A5 also possessed a genomic region harboring ORF2, ORF3, and ORF4 (GenBank accession no. AY130970.1). These four open reading frames are predicted to encode the following proteins: ORF1, a putative glycosyltransferase similar to GtfD, which has been identified as a fucosyltransferase involved in the biosynthesis of serovar 2-specific GPL (73% identity) (30); ORF2, a putative glycosyltransferase, designated GtfTB, showing high homology to Rv1516c of *M. tuberculosis* (61% identity) (28); ORF3, a putative polysaccharide pyruvyltransferase similar to MSMEG_4736 and MSMEG_4737 of *M. smegmatis* (61 and 58% identity, respectively) (GenBank accession no. NC_008596.1); and ORF4, a putative *O*-methyltransferase similar to MSMEG_4739 of *M. smegmatis* (55% identity) (GenBank accession no. NC_008596.1).

Identification of the genes required for synthesis of the sugar residue unique to serovar 8-specific GPL. Based on the deduced functions of the genes in the 4.6-kb fragment, we focused on *gtfTB* (ORF2), ORF3, and ORF4 and characterized them by performing expression analyses. Because the serovar 8-specific GPL has a structure in which the Rha residue of serovar 1-specific GPL is further glycosylated (Table 1), it was necessary to prepare a strain producing serovar 1-specific GPL that could be the substrate for the enzymes participating in the biosynthesis of serovar 8-specific GPL. For this, as previously demonstrated, we created a recombinant *M. smegmatis* strain, designated MS-S1, by introducing the plasmid vector pMV-rtfA having the *M. avium rtfA* gene, which converts nsGPLs to serovar 1-specific GPL (30). We then introduced the integrative expression vector pYM-gtfTB possessing *gtfTB* into MS-S1 and assessed GPL profiles by performing a TLC analysis (Fig. 2). By comparison with the profile of MS-S1/pYM301a (vector control) (Fig. 2, lane A), two new spots, designated spots GPL-SG-U and -D, were observed in MS-S1/pYM-gtfTB (Fig. 2, lane B), indicating that serovar 1-specific

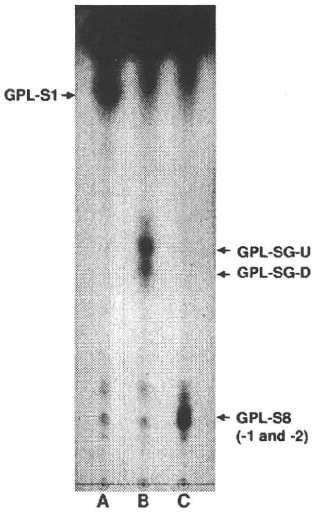

FIG. 2. TLC of crude GPL extracts from recombinant *M. smegmatis* strains MS-S1/pYM301a (A), MS-S1/pYM-gtfTB (B), and MS-S1/pYM-gtfTB-orf3-orf4 (C). GPL extracts were prepared from the total-lipid fraction, and this was followed by mild alkaline hydrolysis. Samples were spotted and developed using $CHCl_3$-CH_3OH-H_2O (30:8:1, vol/vol/vol).

GPL was converted to structurally different compounds by expression of *gtfTB*. Moreover, when the expression vector pYM-gtfTB-orf3-orf4 containing *gtfTB*, ORF3, and ORF4 was introduced into MS-S1, another new spot, designated GPL-S8, appeared (Fig. 2, lane C), implying that the structure of GPL-SG-U and -D was further modified by the products of ORF3 and ORF4. To confirm that these compounds contain the sugar residues associated with serovar 8-specific GPL, we performed a GC-MS analysis of the monosaccharides released from crude GPL extracts of each recombinant strain and the MAC serovar 8 strain (Fig. 3). The results showed that there was an excess of Glc, together with Rha, 6-d-Tal, 3,4-di-*O*-methyl-Rha, and 2,3,4-tri-*O*-methyl-Rha, in the profile of MS-S1/pYM-gtfTB compared with other profiles, as well as minor Glc peaks presumably derived from traces of trehalose-containing glycolipids (Fig. 3B). This indicates that the *gtfTB* gene mediates the transfer of a Glc residue to serovar 1-specific GPL. In contrast, the profile of MS-S1/pYM-gtfTB-orf3-orf4 revealed the presence of 4,6-*O*-(1-carboxyethylidene)-3-*O*-methyl-Glc, which was also detected in the MAC serovar 8 strain (Fig. 3C and D), demonstrating that the three genes are associated with the formation of the unique sugar residue of serovar 8-specific GPL.

Functional characterization of *gtfTB*. Expression analysis showed that serovar 1-specific GPL was converted to new compounds containing Glc when the *gtfTB* gene was expressed (Fig. 2, lane B, and Fig. 3B). Although these results suggested that the product of *gtfTB* participates in the formation of a Glc residue, it is not clear whether *gtfTB* encodes the glycosyltransferase that transfers Glc via 1→3 linkage to the Rha residue of serovar 1-specific GPL, whose linkage was previously detected in serovar 8-specific GPL (7, 8). To elucidate the function of *gtfTB*, we determined the linkage of sugar moieties of GPL-SG-U and -D, which were produced by recombinant strain

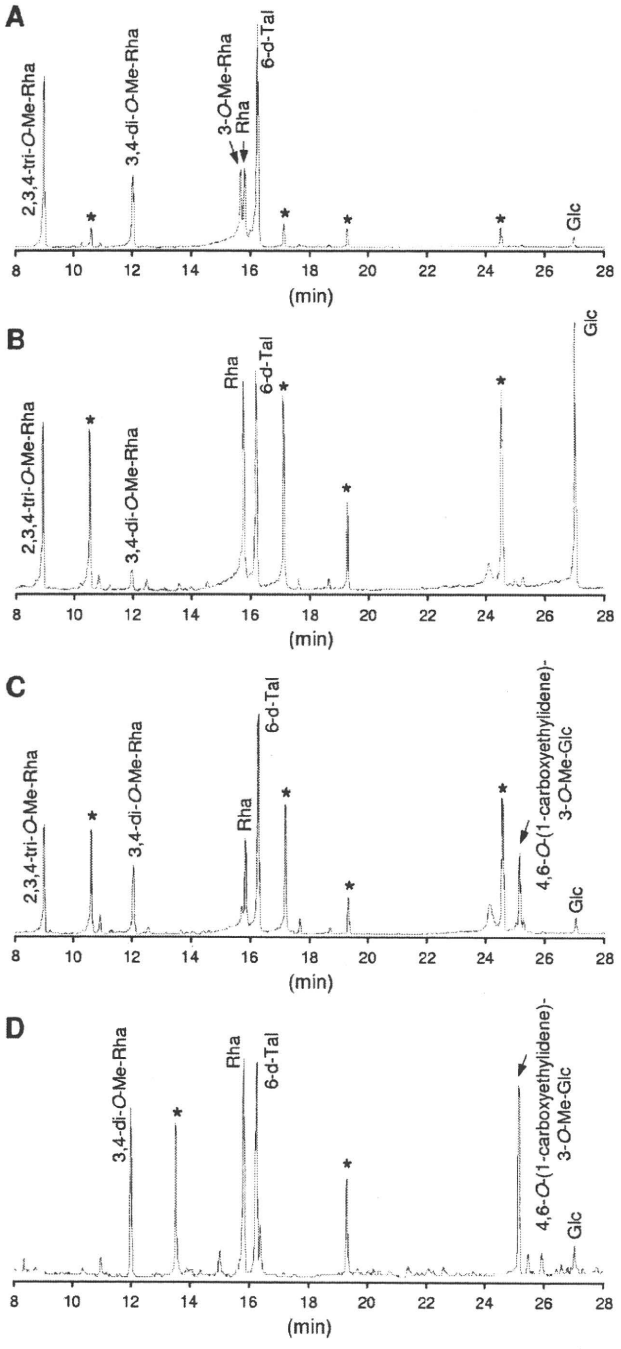

FIG. 3. GC-MS of alditol acetate derivatives from crude GPL extracts of recombinant strains *M. smegmatis* MS-S1/pYM301a (A), MS-S1/pYM-gtfTB (B), and MS-S1/pYM-gtfTB-orf3-orf4 (C) and a MAC serovar 8 strain (D). GPL extracts were prepared from the total-lipid fraction, and this was followed by mild alkaline hydrolysis. Asterisks indicate noncarbohydrates. Me, methyl.

MS-S1/pYM-gtfTB (Fig. 2, lane B). After extraction of the products from the corresponding bands on the TLC plate, purified GPL-SG-U and -D were subjected to perdeuteriomethylation followed by GC-MS. The differences in the TLC profiles of GPL-SG-U and -D might have been due to the presence or absence of fatty acid methylation, which is often observed in *M. smegmatis* GPLs (23, 31), whereas the GC-MS profiles and fragmentation ions for GPL-SG-U and -D were identical, demonstrating that GPL-SG-U and -D had the same sugar moieties and linkages. Therefore, the profiles of GPL-SG-U shown here are representative of GPL-SG-U and -D. The GC-MS profile of GPL-SG-U contained four peaks corresponding to 6-d-Tal, Rha, Glc, and 2,3,4-tri-*O*-methyl-Rha (data not shown). The characteristic spectra for Glc, Rha, and 6-d-Tal are shown in Fig. 4. The spectrum of Glc had fragment ions at *m/z* 121, 167, and 168, which represent the presence of deuteriomethyl groups at positions C-2, C-3, and C-4 (Fig. 4A). In contrast, fragment ions at *m/z* 121, 134, 193, and 240 were detected for Rha, indicating that a deuteriomethyl group was introduced at positions C-2 and C-4 of Rha, in which position C-3 was acetylated (Fig. 4B). In addition, detection of fragment ions at *m/z* 134, 181, and 193 (Fig. 4C) revealed that there was deuteriomethylation at positions C-3 and C-4 in 6-d-Tal. These results demonstrated that position C-1 of Glc is linked to position C-3 of Rha but not to position C-2 of 6-d-Tal, because it has been determined previously that position C-1 of Rha is linked to position C-2 of 6-d-Tal in the oligosaccharide of serovar 1-specific GPL (17). Accordingly, the oligosaccharide structures of GPL-SG-U and -D were determined to have Glc-(1→3)-Rha-(1→2)-6-d-Tal at D-*allo*-Thr, demonstrating that *gtfTB* encodes the glucosyltransferase that transfers a Glc residue via 1→3 linkage to the Rha residue of serovar 1-specific GPL.

Structural assignment of GPL-S8 synthesized by expression of *gtfTB*, ORF3, and ORF4. GC-MS of the crude GPL extract from MS-S1/pYM-gtfTB-orf3-orf4 revealed the presence of 4,6-*O*-(1-carboxyethylidene)-3-*O*-methyl-Glc (Fig. 3C). To confirm that this structural component was derived from GPL-S8, we performed GC-MS and MALDI-TOF MS analyses of purified GPL-S8. The results showed that GPL-S8 contained a 4,6-*O*-(1-carboxyethylidene)-3-*O*-methyl-Glc residue and two main pseudomolecular ions (*m/z* 1,565.9 and 1,579.8 $[M + Na]^+$) (data not shown). Consequently, as shown in Fig. 5, these results were consistent with the proposed structure for GPL-S8-1 and -2 containing 4,6-*O*-(1-carboxyethylidene)-3-*O*-methyl-Glc, with differences in pseudomolecular ions due to fatty acid methylation.

DISCUSSION

Structural diversity of the ssGPLs, notably in their sugar residues, defines 28 serovars of MAC. Although these ssGPLs are known to contribute to the virulence of MAC, the mechanisms of their biosynthetic regulation are largely unknown. In this study, we clarified the biosynthetic pathway for serovar 8-specific GPL, specifically the glycosylation step in which a Glc residue is transferred to the Rha residue of serovar 1-specific GPL.

To isolate the genomic region associated with the biosynthesis of serovar 8-specific GPL, we compared the GPL biosynthetic gene clusters in several MAC strains and found significant differences in the *gtfB-drrC* region. The segment flanking the 3′ end of the *gtfB-drrC* region includes several genes responsible for the serovar 1-specific GPL whose structure is found in all ssGPLs. On the other hand, it is experimentally

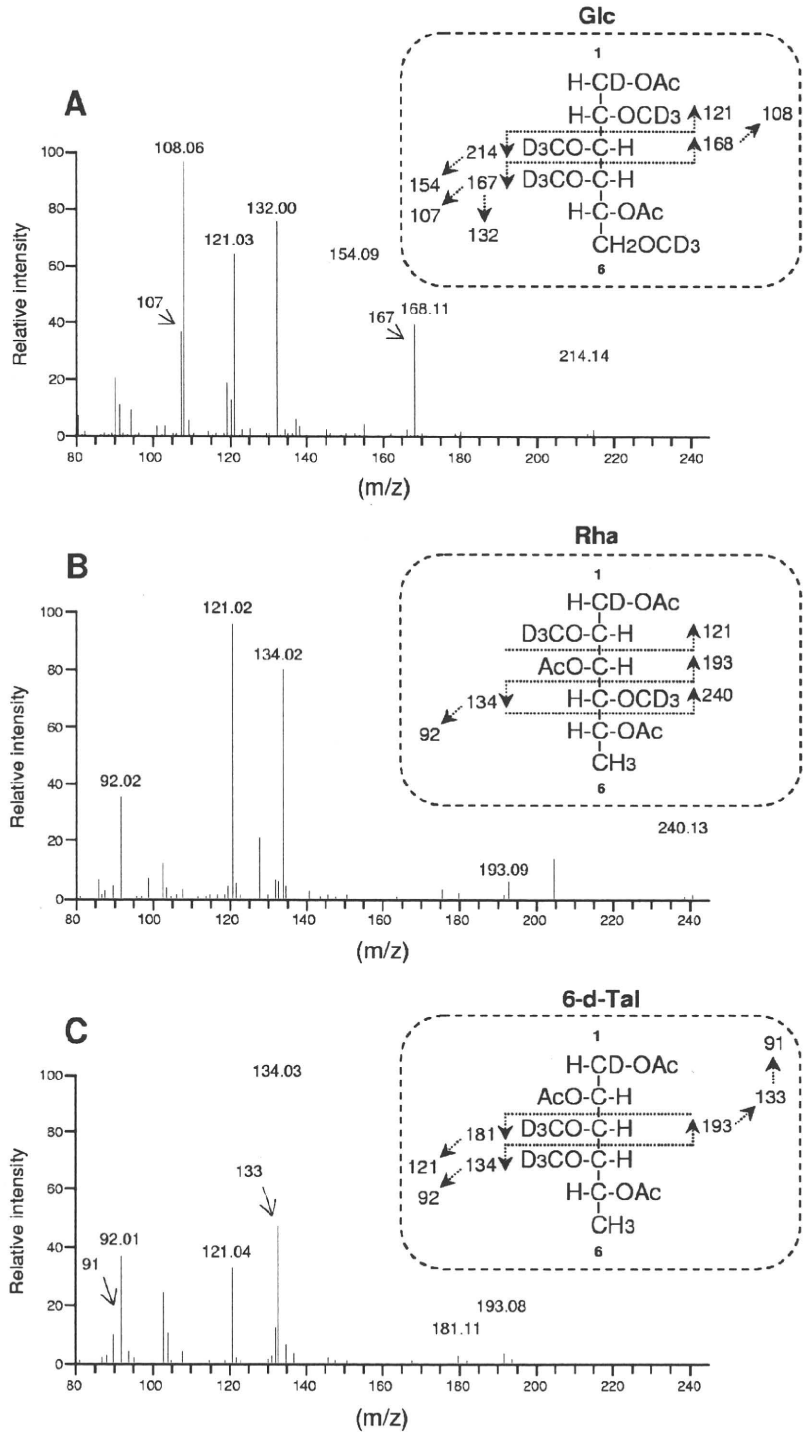

FIG. 4. GC-MS spectra and fragment ion assignments for Glc (A), Rha (B), and 6-d-Tal (C), which were derived from alditol acetates of sugars released from deuteriomethylated GPL-SG-U. Ac, acetate; D, deuterium.

clarified that the *gtfB-drrC* regions of serovar 2-, 7-, and 16-specific GPL-producing strains contain the genes involved in the formation of the specific sugar residues that are transferred to the Rha residue of serovar 1-specific GPL (18, 19, 30). Thus, this region could play an important role in generating the structural diversity of ssGPLs. As shown in this study, the specific functions for formation of sugar moieties of serovar 8-specific GPL were due to the genes present in the *gtfB-drrC*

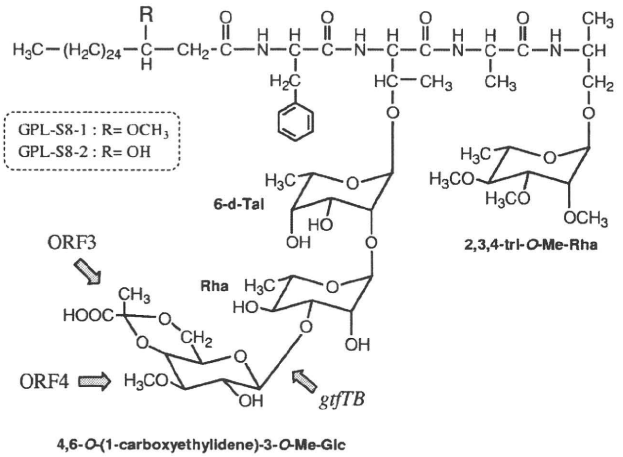

FIG. 5. Proposed structure and biosynthetic genes of GPL-S8 (serovar 8-specific GPL). Me, methyl.

region, suggesting that focusing on this region might provide clues for elucidating the characteristics of other ssGPLs whose biosynthesis is still not known.

It has been reported previously that the *gtfTB* gene in *M. avium* strains 104 and A5 was not likely to be associated with GPL biosynthesis because its ancestral homologue, Rv1516c (61% identity with the GtfTB gene), was the gene of *M. tuberculosis*, which produces no GPLs (28). Thus, it was interesting that *gtfTB* encodes a glycosyltransferase that does participate in GPL biosynthesis in which a Glc residue is transferred to serovar 1-specific GPL, yielding the serovar 8-specific GPL. *M. avium* strains 104 and A5 synthesize serovar 1-specific GPL as a final product and intermediate, respectively, while it has been recognized that neither of these strains produces serovar 8-specific GPL in spite of the presence of *gtfTB* in the GPL biosynthetic gene cluster (28). These observations raised the possibility that the transcription of *gtfTB* is inefficient in both strains due to the upstream sequences. Actually, in *M. avium* strain 104, a transposase sequence was observed upstream of *gtfTB*, indicating that this strain might be deficient in glucosylation, and consequently a serovar 1-specific GPL-producing strain is obtained (28). On the other hand, it has been shown that the biosynthetic gene cluster for serovar 7-specific GPL in *M. intracellulare* strain ATCC 35847 contains a putative glycosyltransferase gene which encodes amino acid sequences that are similar to the amino acid sequences encoded by *gtfTB* (59% identity) (18). Structural analysis of sugar moieties in serovar 7-specific GPL indicated that this GtfTB homologue may serve as a glycosyltransferase during formation of the terminal amidohexose residue that structurally resembles Glc (18).

The deduced amino acid sequences encoded by ORF3 and ORF4 showed that these genes putatively encode polysaccharide pyruvyltransferase and *O*-methyltransferase, respectively. Expression of ORF3 and ORF4 together with *gtfTB* led to structural alterations in which Glc was modified with both 4,6-*O*-(1-carboxyethylidene) and 3-*O*-methyl groups. Based on these observations, it is strongly suggested that ORF3 is associated with the formation of the 4,6-*O*-(1-carboxyethylidene) group that is synonymous with the cyclic pyruvate ketal and that ORF4 is associated with the 3-*O*-methylation of the Glc residue (Fig. 5). In mycobacteria, homologues of ORF3 and ORF4 were found only in *M. smegmatis*, as MSMEG_4736 (for ORF3), MSMEG_4737 (for ORF3), and MSMEG_4739 (for ORF4). *M. smegmatis* also produces glycolipids containing 4,6-*O*-(1-carboxyethylidene)-3-*O*-methyl-Glc as a sugar moiety (25, 34), which suggests that both homologues participate in the synthesis of these glycolipids. Sugar residues with a 4,6-*O*-(1-carboxyethylidene) group substitution have been found in carbohydrates such as extracellular polysaccharide and N-linked glycan, which are produced by some bacteria and yeasts (1, 15, 20, 22, 26). It has been shown that an increase in 4,6-*O*-(1-carboxyethylidene)-containing sugar residues leads to enhanced viscosity of extracellular polysaccharide from *Xanthomonas* sp., which alters the cell surface properties related to cellular attachment and protection from environmental stress (10). Accordingly, in terms of the properties of serovar 8-specific GPL, the presence of the 4,6-*O*-(1-carboxyethylidene) group might influence the pathogenicity of MAC serovar 8.

With regard to the antibody reactivity, it is unclear whether serovar 8-specific antibodies react with GPL-S8 because there are minor structural differences in the methylated positions of fatty acids and the terminal Rha residue linked to the tetrapeptide between GPL-S8 and serovar 8-specific GPL of MAC. Evaluation of the antibody response to GPL-S8 using serovar 8-specific antibodies would facilitate understanding the immunoreactivity mediated by ssGPLs.

In this study, we proved that *gtfTB* and adjacent genes in the GPL biosynthetic gene cluster in MAC serovar 8 strain are responsible for the formation of a unique glucose residue in serovar 8-specific GPL (Fig. 5). In particular, *gtfTB* encodes the glucosyltransferase that plays a critical role in the pathway leading from serovar 1-specific GPL to serovar 8-specific GPL. Through further study, including generation of *gtfTB* knockout mutants of MAC serovar 8 strains, results relevant to the biosynthesis of serovar 8-specific GPL might help clarify the biological function of ssGPLs and their role in the host-pathogen relationships of MAC.

ACKNOWLEDGMENTS

This study was supported in part by a Grant-in-Aid for Young Scientists (B) from the Ministry of Education, Culture, Science and Technology of Japan and Research on Emerging and Re-Emerging Infectious Diseases from the Ministry of Health, Labor and Welfare of Japan.

REFERENCES

1. **Aman, P., M. McNeil, L.-E. Franzen, A. G. Darvill, and P. Albersheim.** 1981. Structural elucidation, using HPLC-MS and GLC-MS, of the acidic exopolysaccharide secreted by *Rhizobium meliloti* strain Rm1021. Carbohydr. Res. **95**:263–282.
2. **Aspinall, G. O., D. Chatterjee, and P. J. Brennan.** 1995. The variable surface glycolipids of mycobacteria: structures, synthesis of epitopes, and biological properties. Adv. Carbohydr. Chem. Biochem. **51**:169–242.
3. **Barrow, W. W., T. L. Davis, E. L. Wright, V. Labrousse, M. Bachelet, and N. Rastogi.** 1995. Immunomodulatory spectrum of lipids associated with *Mycobacterium avium* serovar 8. Infect. Immun. **63**:126–133.
4. **Belisle, J. T., K. Klaczkiewicz, P. J. Brennan, W. R. Jacobs, Jr., and J. M. Inamine.** 1993. Rough morphological variants of *Mycobacterium avium*. Characterization of genomic deletions resulting in the loss of glycopeptidolipid expression. J. Biol. Chem. **268**:10517–10523.
5. **Bhatnagar, S., and J. S. Schorey.** 2007. Exosomes released from infected macrophages contain *Mycobacterium avium* glycopeptidolipids and are proinflammatory. J. Biol. Chem. **282**:25779–25789.
6. **Bjorndal, H., C. G. Hellerqvist, B. Lindberg, and S. Svensson.** 1970. Gas-liquid chromatography and mass spectrometry in methylation analysis of polysaccharides. Angew. Chem. Int. Ed. Engl. **9**:610–619.

7. **Brennan, P. J., G. O. Aspinall, and J. E. Shin.** 1981. Structure of the specific oligosaccharides from the glycopeptidolipid antigens of serovars in the *Mycobacterium avium-Mycobacterium intracellulare-Mycobacterium scrofulaceum* complex. J. Biol. Chem. **256**:6817–6822.
8. **Brennan, P. J., H. Mayer, G. O. Aspinall, and J. E. Nam Shin.** 1981. Structures of the glycopeptidolipid antigens from serovars in the *Mycobacterium avium/Mycobacterium intracellulare/Mycobacterium scrofulaceum* serocomplex. Eur. J. Biochem. **115**:7–15.
9. **Brennan, P. J., and H. Nikaido.** 1995. The envelope of mycobacteria. Annu. Rev. Biochem. **64**:29–63.
10. **Casas, J. A., V. E. Santos, and F. Garcia-Ochoa.** 2000. Xanthan gum production under several operational conditions: molecular structure and rheological properties. Enzyme Microb. Technol. **26**:282–291.
11. **Chatterjee, D., and K. H. Khoo.** 2001. The surface glycopeptidolipids of mycobacteria: structures and biological properties. Cell. Mol. Life Sci. **58**: 2018–2042.
12. **Ciucanu, I., and F. Kerek.** 1984. A simple and rapid method for the permethylation of carbohydrates. Carbohydr. Res. **131**:209–217.
13. **Daffe, M., and P. Draper.** 1998. The envelope layers of mycobacteria with reference to their pathogenicity. Adv. Microb. Physiol. **39**:131–203.
14. **Daffe, M., M. A. Laneelle, and G. Puzo.** 1983. Structural elucidation by field desorption and electron-impact mass spectrometry of the C-mycosides isolated from *Mycobacterium smegmatis*. Biochim. Biophys. Acta **751**:439–443.
15. **D'Haeze, W., J. Glushka, R. De Rycke, M. Holsters, and R. W. Carlson.** 2004. Structural characterization of extracellular polysaccharides of *Azorhizobium caulinodans* and importance for nodule initiation on *Sesbania rostrata*. Mol. Microbiol. **52**:485–500.
16. **Eckstein, T. M., J. T. Belisle, and J. M. Inamine.** 2003. Proposed pathway for the biosynthesis of serovar-specific glycopeptidolipids in *Mycobacterium avium* serovar 2. Microbiology **149**:2797–2807.
17. **Eckstein, T. M., F. S. Silbaq, D. Chatterjee, N. J. Kelly, P. J. Brennan, and J. T. Belisle.** 1998. Identification and recombinant expression of a *Mycobacterium avium* rhamnosyltransferase gene (*rtfA*) involved in glycopeptidolipid biosynthesis. J. Bacteriol. **180**:5567–5573.
18. **Fujiwara, N., N. Nakata, S. Maeda, T. Naka, M. Doe, I. Yano, and K. Kobayashi.** 2007. Structural characterization of a specific glycopeptidolipid containing a novel *N-acyl*-deoxy sugar from *Mycobacterium intracellulare* serotype 7 and genetic analysis of its glycosylation pathway. J. Bacteriol. **189**:1099–1108.
19. **Fujiwara, N., N. Nakata, T. Naka, I. Yano, M. Doe, D. Chatterjee, M. McNeil, P. J. Brennan, K. Kobayashi, M. Makino, S. Matsumoto, H. Ogura, and S. Maeda.** 2008. Structural analysis and biosynthesis gene cluster of an antigenic glycopeptidolipid from *Mycobacterium intracellulare*. J. Bacteriol. **190**:3613–3621.
20. **Gemmill, T. R., and R. B. Trimble.** 1996. *Schizosaccharomyces pombe* produces novel pyruvate-containing N-linked oligosaccharides. J. Biol. Chem. **271**:25945–25949.
21. **Horgen, L., E. L. Barrow, W. W. Barrow, and N. Rastogi.** 2000. Exposure of human peripheral blood mononuclear cells to total lipids and serovar-specific glycopeptidolipids from *Mycobacterium avium* serovars 4 and 8 results in inhibition of TH1-type responses. Microb. Pathog. **29**:9–16.
22. **Jansson, P. E., L. Kenne, and B. Lindberg.** 1975. Structure of extracellular polysaccharide from *Xanthomonas campestris*. Carbohydr. Res. **45**:275–282.
23. **Jeevarajah, D., J. H. Patterson, M. J. McConville, and H. Billman-Jacobe.** 2002. Modification of glycopeptidolipids by an *O*-methyltransferase of *Mycobacterium smegmatis*. Microbiology **148**:3079–3087.
24. **Julander, I., S. Hoffner, B. Petrini, and L. Ostlund.** 1996. Multiple serovars of *Mycobacterium avium* complex in patients with AIDS. APMIS **104**:318–320.
25. **Kamisango, K., S. Saadat, A. Dell, and C. E. Ballou.** 1985. Pyruvylated glycolipids from *Mycobacterium smegmatis*. Nature and location of the lipid components. J. Biol. Chem. **260**:4117–4121.
26. **Kojima, N., S. Kaya, Y. Araki, and E. Ito.** 1988. Pyruvic-acid-containing polysaccharide in the cell wall of *Bacillus polymyxa* AHU 1385. Eur. J. Biochem. **174**:255–260.
27. **Krzywinska, E., S. Bhatnagar, L. Sweet, D. Chatterjee, and J. S. Schorey.** 2005. *Mycobacterium avium* 104 deleted of the methyltransferase D gene by allelic replacement lacks serotype-specific glycopeptidolipids and shows attenuated virulence in mice. Mol. Microbiol. **56**:1262–1273.
28. **Krzywinska, E., and J. S. Schorey.** 2003. Characterization of genetic differences between *Mycobacterium avium* subsp. *avium* strains of diverse virulence with a focus on the glycopeptidolipid biosynthesis cluster. Vet. Microbiol. **91**:249–264.
29. **Li, Z., G. H. Bai, C. F. von Reyn, P. Marino, M. J. Brennan, N. Gine, and S. L. Morris.** 1996. Rapid detection of *Mycobacterium avium* in stool samples from AIDS patients by immunomagnetic PCR. J. Clin. Microbiol. **34**:1903–1907.
30. **Miyamoto, Y., T. Mukai, Y. Maeda, N. Nakata, M. Kai, T. Naka, I. Yano, and M. Makino.** 2007. Characterization of the fucosylation pathway in the biosynthesis of glycopeptidolipids from *Mycobacterium avium* complex. J. Bacteriol. **189**:5515–5522.
31. **Miyamoto, Y., T. Mukai, N. Nakata, Y. Maeda, M. Kai, T. Naka, I. Yano, and M. Makino.** 2006. Identification and characterization of the genes involved in glycosylation pathways of mycobacterial glycopeptidolipid biosynthesis. J. Bacteriol. **188**:86–95.
32. **Miyamoto, Y., T. Mukai, F. Takeshita, N. Nakata, Y. Maeda, M. Kai, and M. Makino.** 2004. Aggregation of mycobacteria caused by disruption of fibronectin-attachment protein-encoding gene. FEMS Microbiol. Lett. **236**:227–234.
33. **Patterson, J. H., M. J. McConville, R. E. Haites, R. L. Coppel, and H. Billman-Jacobe.** 2000. Identification of a methyltransferase from *Mycobacterium smegmatis* involved in glycopeptidolipid synthesis. J. Biol. Chem. **275**:24900–24906.
34. **Saadat, S., and C. E. Ballou.** 1983. Pyruvylated glycolipids from *Mycobacterium smegmatis*. Structures of two oligosaccharide components. J. Biol. Chem. **258**:1813–1818.
35. **Snapper, S. B., R. E. Melton, S. Mustafa, T. Kieser, and W. R. Jacobs, Jr.** 1990. Isolation and characterization of efficient plasmid transformation mutants of *Mycobacterium smegmatis*. Mol. Microbiol. **4**:1911–1919.
36. **Stover, C. K., V. F. de la Cruz, T. R. Fuerst, J. E. Burlein, L. A. Benson, L. T. Bennett, G. P. Bansal, J. F. Young, M. H. Lee, G. F. Hatfull, S. B. Snapper, R. G. Barletta, W. R. Jacobs, Jr., and B. R. Bloom.** 1991. New use of BCG for recombinant vaccines. Nature **351**:456–460.
37. **Sweet, L., and J. S. Schorey.** 2006. Glycopeptidolipids from *Mycobacterium avium* promote macrophage activation in a TLR2- and MyD88-dependent manner. J. Leukoc. Biol. **80**:415–423.
38. **Tassell, S. K., M. Pourshafie, E. L. Wright, M. G. Richmond, and W. W. Barrow.** 1992. Modified lymphocyte response to mitogens induced by the lipopeptide fragment derived from *Mycobacterium avium* serovar-specific glycopeptidolipids. Infect. Immun. **60**:706–711.
39. **Tsang, A. Y., J. C. Denner, P. J. Brennan, and J. K. McClatchy.** 1992. Clinical and epidemiological importance of typing of *Mycobacterium avium* complex isolates. J. Clin. Microbiol. **30**:479–484.
40. **Vergne, I., and M. Daffe.** 1998. Interaction of mycobacterial glycolipids with host cells. Front. Biosci. **3**:d865–876.
41. **Yakrus, M. A., and R. C. Good.** 1990. Geographic distribution, frequency, and specimen source of *Mycobacterium avium* complex serotypes isolated from patients with acquired immunodeficiency syndrome. J. Clin. Microbiol. **28**:926–929.